Department of Chemistry
University of Helsinki
Finland

Hyaluronic acid graft copolymers as potential vehicles for intravitreal drug delivery

Tina Borke

ACADEMIC DISSERTATION

To be presented, with the permission of the Faculty of Science of the University of Helsinki, for public examination in auditorium A129, Department of Chemistry, on May 25th 2018, at 12 noon.

Helsinki 2018

Supervisors

Dr. Sami Hietala and Professor Heikki Tenhu
Department of Chemistry
University of Helsinki
Finland

Opponent

Professor Béla Iván
Institute of Materials and Environmental Chemistry
Research Centre for Natural Sciences
Hungarian Academy of Science
Hungary

Reviewers

Professor Eva Malmström Jonsson
Department of Fibre and Polymer Technology
School of Engineering Sciences in Chemistry, Biotechnology and Health
KTH Royal Institute of Technology
Sweden

Professor Carl-Eric Wilén
Laboratory of Polymer Technology
Faculty of Science and Engineering
Åbo Akademi University
Finland

ISBN 978-951-51-4199-6 (paperback)
ISBN 978-951-51-4200-9 (PDF)
https://ethesis.helsinki.fi

Unigrafia
Helsinki 2018

Abstract

Water-soluble polymers are promising drug carrier materials. Especially polysaccharide graft copolymers are desirable for this purpose as they combine the favorable features of biopolymers, such as biocompatibility and biodegradability, with the controlled structure and functionality of synthetic polymers. This thesis examines water-soluble hyaluronic acid (HA) graft copolymers with cleavable arms as potential vehicles for sustained intravitreal drug delivery.

Retinal diseases are the leading cause of visual impairment in the aging Western societies, but drug delivery to the back of the eye is complicated by multiple barriers. Intravitreal injections so far yield the highest bioavailability of drugs, however they need to be repeated frequently due to the rapid clearance of the therapeutics. Sustained delivery of drugs over extended periods of time is a promising strategy to prolong the injection intervals. Macromolecular drug delivery vehicles can help to reduce the clearance rate due to their high molecular weight and low diffusivity.

The studied graft copolymers are based on a high molecular weight HA backbone and poly(glyceryl glycerol) (PGG) side chains attached via hydrolysable linkers. HA is a natural constituent of the vitreous and used to prolong the vehicle's retention time in the eye. PGG is a multihydroxyfunctional polyether featuring a poly(ethylene glycol) (PEG) backbone and pendant 1,2-diol moieties in every repeating unit. As such, PGG possesses similar biocompatibility and antifouling properties as PEG, while being amenable to the conjugation of multiple drugs, probes and targeting moieties.

HA was functionalized with hydrolysable alkynyl linkers for use in click grafting. The effect of modifications (*i.e.* amidation, esterification and click reaction) on HA properties was studied and the reaction conditions were optimized to minimize degradation while achieving efficient derivatization. Azido-functional PGG was prepared by ring-opening polymerization of epoxide monomers. Functionalization of PGG hydroxyl groups was explored to establish strategies for conjugation of drugs, probes and targeting molecules. For example, PGG could be efficiently labeled with rhodamine B boronic acid, due to formation of reversible boronic esters with the pendant 1,2-diol moieties. HA-PGG graft copolymers were prepared by copper-mediated azide-alkyne cycloaddition (CuAAC).

The synthesized materials were studied under simulated physiological conditions to determine their stability and the cleavage of hydrolysable bonds. The HA backbone was stable during one month of incubation in buffer or vitreous liquid. The polymer-from-polymer release of PGG grafts from the HA-PGG ester copolymer was investigated and the hydrolysis rates were quantified. Hydrolytic cleavage of PGG chains from HA was significantly slower than cleavage of the small molecular weight alkynyl linkers, and was attributed to steric crowding at the ester bond. Hence, graft copolymers with cleavable arms have the potential to achieve longer lasting release than polymeric prodrugs with drugs attached directly to the backbone.

The biocompatibility of PGG and HA-PGG copolymers was tested in cell cultures. The materials exhibited similar levels of cell viability as polyvinyl alcohol, which is FDA-approved for ocular applications.

Acknowledgements

The present study was conducted at the Department of Chemistry, University of Helsinki, during the years 2012-2018 and was funded by the Academy of Finland (grant number 263573) and the Doctoral Program in Chemistry and Molecular Science, University of Helsinki.

I wish to express my deepest gratitude to my supervisor Dr. Sami Hietala, who was always available when I needed help, cheered me up in the face of failed reactions and supported me in every way possible. I am also very grateful to Prof. Heikki Tenhu for enabling me to perform and conclude this work at the University of Helsinki.

Further, I wish to acknowledge the contribution of my collaborators: Prof. Françoise Winnik, Prof. Arto Urtti, Dr. Madhushree Bhattacharya, Dr. Polina Ilina, Antti Korpi, and Mathie Najberg. Thank you for your help and valuable input.

I am grateful to Prof. Eva Malmström Jonsson and Prof. Carl-Eric Wilén for taking the time to examine my thesis and to Prof. Béla Iván for traveling all the way to Finland to be my opponent.

Special thanks go to Prof. Sirkka-Liisa Maunu, Seija Lemettinen, Juha Solasaari, Dr. Vladimir Aseyev, and Ennio Zuccaro for their support throughout the years. I also wish to thank all my colleagues for the vivid discussions during coffee breaks and the great atmosphere we had in the lab. I especially want to acknowledge my long time office mate and all-round troubleshooter, Sami-Pekka. Thanks for everything. Also, many thanks to all former and current members of HYPPY ry for the great events, we organized together, and all the memories we made.

Tiefer Dank gebührt meinen Eltern. Euer Zuspruch und Eure Unterstützung von klein auf hat dazu geführt, dass mir noch keine Aufgabe zu unlösbar erschien und ohne Euch hätte ich dieses Auslandsabenteuer vermutlich nicht angehen können. Des Weiteren danke ich der gesamten (erweiterten) Familie Pooch, die mich so herzlich in Ihrer Mitte aufgenommen hat und bei dieser Unternehmung genauso mit mir mitfieberte, wie mit Ihrem Fabi.

Zu guter Letzt und aus tiefstem Herzen danke ich meinem Verlobten, Seelenverwandten und Lieblingskollegen, Fabian. Du bist das Licht, dass meine Mittagspausen, Konferenz-reisen und Feierabende erhellt. Vielen Dank für die Diskussionen, Inspirationen und Aufmunterungen, die maßgeblich zum Erfolg dieser Arbeit beigetragen haben.

Tina Borke
Helsinki, April 2018

Contents

List of original publications

This thesis is based on the following publications:

I Borke, T.; Winnik, F. M.; Tenhu, H.; Hietala, S. **Optimized Triazine-Mediated Amidation for Efficient and Controlled Functionalization of Hyaluronic Acid.** *Carbohydrate Polymers* **2015**, *116*, 42–50. DOI: 10.1016/j.carbpol.2014.04.012.

II Borke, T.; Korpi, A.; Pooch, F.; Tenhu, H.; Hietala, S. **Poly(Glyceryl Glycerol): A Multi-Functional Hydrophilic Polymer for Labeling with Boronic Acids.** *J. Polym. Sci. Part A: Polym. Chem.* **2017**, *55* (11), 1822–1830. DOI: 10.1002/pola.28497.

III Borke, T.; Najberg, M.; Ilina, P.; Bhattacharya, M.; Urtti, A.; Tenhu, H.; Hietala, S. **Hyaluronic Acid Graft Copolymers with Cleavable Arms as Potential Intravitreal Drug Delivery Vehicles.** *Macromol. Biosci.* **2018**, *18* (1), 1700200. DOI: 10.1002/mabi.201700200.

The publications are referred to in the text by their roman numerals.

The author's contribution to the publications:
For all publications T. Borke has designed the research plan, synthesized most of the materials, conducted the experiments (except the cell studies) and analyzed the data. Borke independently wrote the first drafts of the manuscripts and finalized them together with the co-authors.

Abbreviations

adj. R^2	coefficient of determination adjusted by the degrees of freedom
Al-*i*Bu_3	triisobutylaluminum
AMD	age-related macular degeneration
AROP	anionic ring-opening polymerization
ARPE-19	human retinal pigment epithelial cells
ATRP	atom-transfer radical polymerization
CROP	cationic ring-opening polymerization
CuAAC	copper-mediated azide-alkyne cycloaddition
CV-1	monkey kidney fibroblast cells
D_2O	deuterium oxide
DBU	1,8-diazabicyclo[5.4.0]undec-7-ene
DCC	*N,N'*-dicyclohexylcarbodiimide
DMAP	4-dimethylaminopyridine
DMF	dimethylformamide
DMSO	dimethyl sulfoxide
DMSO-d_6	deuterated dimethyl sulfoxide
DMT-MM	4-(4,6-dimethoxy-1,3,5-triazin-2-yl)-4-methylmorpholinium chloride
DMT-OH	2-hydroxy-4,6-dimethoxy-1,3,5-triazine
DNA	deoxyribonucleic acid
DOPE	1,2-dioleoyl-*sn*-glycero-3-phosphoethanolamine
DOSY	diffusion-ordered NMR spectroscopy
DP	degree of polymerization
DS	degree of substitution
EDC	1-ethyl-3-(3-dimethylaminopropyl)carbodiimide
EDTA	ethylenediaminetetraacetic acid
ELM	external limiting membrane
eq.	equivalent
Fab	antigen-binding region of an antibody
FDA	U.S. Food and Drug Administration
FRP	free radical polymerization
FT-IR	Fourier transform infrared spectroscopy
HA	hyaluronic acid
HOBt	1-hydroxybenzotriazole
HSQC	heteronuclear single quantum coherence NMR spectroscopy
HUVEC	human umbilical vein endothelial cells
IGG	(DL-1,2-isopropylidene glyceryl) glycidyl ether
ILM	inner limiting membrane
k_{diff}	diffusion rate constant
k_{hydr}	hydrolysis rate constant
LE	labeling efficiency
MeOD	deuterated methanol
M_n	number-average molecular weight

MTT	3-(4,5-dimethylthiazol-2-yl)-2,5-diphenyltetrazolium bromide
MWCO	molecular weight cut-off
N_3-PGG	α-azido-poly(glyceryl glycerol)
NBu_4I	tetrabutylammonium iodide
NBu_4N_3	tetrabutylammonium azide
NHS	*N*-hydroxysuccinimide
NMR	nuclear magnetic resonance spectroscopy
$NOct_4Br$	tetraoctylammonium bromide
PAMAM	polyamidoamine
PBA	phenylboronic acid
PBS	phosphate-buffered saline
PDI	polydispersity index
PDMAEMA	poly(2-(dimethylamino)ethyl methacrylate)
PEG	poly(ethylene glycol)
PEI	poly(ethylene imine)
PG	polyglycerol
PGG	poly(glyceryl glycerol)
PHPMA	poly(*N*-(2-hydroxypropyl) methacrylamide
PIGG	poly((DL-1,2-isopropylidene glyceryl) glycidyl ether)
PLLA	poly(L-lactide)
PMDETA	*N,N,N',N'',N''*-pentamethyldiethylenetriamine
PNIPAM	poly(*N*-isopropylacrylamide)
PVA	polyvinyl alcohol
RAFT	reversible addition-fragmentation chain-transfer polymerization
RGD	arginyl-glycyl-aspartic acid
ROMP	ring-opening metathesis polymerization
ROP	ring-opening polymerization
RPE	retinal pigment epithelium
SA:V	surface area-to-volume ratio
SEC	size exclusion chromatography
SKOV-3	human ovarian adenocarcinoma cells
$t_{1/2}$	half-life
TBA	tetrabutylammonium
TEA	triethylamine
THF	tetrahydrofuran
UV	ultraviolet

1 Introduction

1.1 Water-soluble polymers as drug carriers

Water-soluble polymers have long been recognized for their potential as drug carriers.[1–3] In 1975, Helmut Ringsdorf described the ideal structure of such a carrier.[4] It consists of a water-soluble, non-toxic polymer backbone with drugs attached via degradable spacers that facilitate their release under predefined conditions and targeting moieties that induce specific interactions at the disease site (Figure 1a). Compared with small drugs, these polymer-drug conjugates exhibit significantly different pharmacokinetic and pharmacodynamic properties (Figure 1b).[5] The most important properties are improved solubility and retarded excretion from the body, which is affected by the high molecular weight.[4]

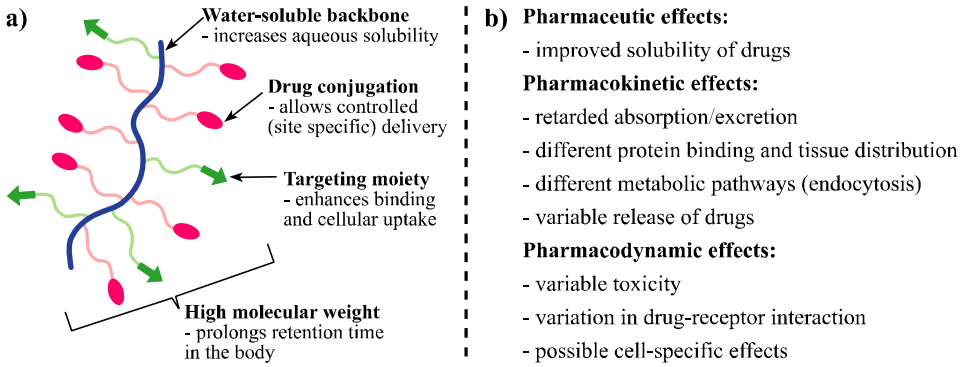

Figure 1 *a) Schematic of an ideal water-soluble polymeric drug carrier redrawn from reference 6. b) Effects of the structure of polymer-drug conjugates on the phases of drug action.*[4]

Both synthetic and natural polymers have been used as drug carriers. They include poly(ethylene glycol) (PEG), poly(*N*-(2-hydroxypropyl) methacrylamide (PHPMA), polyamidoamine (PAMAM), dextran, chitosan and carboxymethylcellulose.[7,8] While synthetic polymers, such as PHPMA, are easy to prepare and modify, their usable molecular weight range is limited. Non-degradable polymers of sizes larger than the renal threshold (~$5 \cdot 10^4$ g mol^{-1}) accumulate in the body.[9] Biopolymers, such as polysaccharides, are naturally high in molecular weight (up to 10^7 g mol^{-1}) and besides are biocompatible and biodegradable.[10] On the other hand, polysaccharides are often difficult to modify and have a limited number of drug attachment sites, if their structural and functional integrity is to be preserved.[11]

A combination of synthetic and natural polymers, as in polysaccharide graft copolymers, overcomes the limitations of the individual components to achieve very high molecular weight and degradability into smaller fragments suitable for renal clearance.

Furthermore, grafting of polysaccharides with synthetic polymers is a way to introduce diverse functionalities while maintaining the bioactive properties of the polysaccharide by a low grafting density.

1.1.1 Polysaccharide graft copolymers

Polysaccharide graft copolymers are prepared by either grafting of ready-made synthetic polymers *onto* a polysaccharide backbone[12–14] or by polymerization *from* the polysaccharide[11,15,16] (Figure 2). With the g*rafting onto* approach, both backbone and side chain polymers can be tailor-made and characterized prior to coupling, but the grafting density is typically limited due to steric hindrance.[17] With g*rafting from*, high grafting densities and narrow molecular weight distributions are achieved, but the side chain lengths are less controlled.[11] Both methods lead to copolymers that can display new functional properties,[18] improved solubility,[19] or response to environmental changes.[20] For example, cationic polysaccharide graft copolymers with positively charged chitosan backbone or cationic poly(2-(dimethylamino)ethyl methacrylate) (PDMAEMA) side chains are investigated for gene delivery applications, because of their ability to complex negatively charged DNA fragments.[21,22] Thermoresponsive graft copolymers of dextran, chitosan or carboxymethylcellulose with poly(*N*-isopropylacrylamide) (PNIPAM) are used to encapsulate drugs,[23,24] while hyaluronic acid-*g*-PNIPAM is widely studied as injectable hydrogel scaffold for tissue engineering.[25–27]

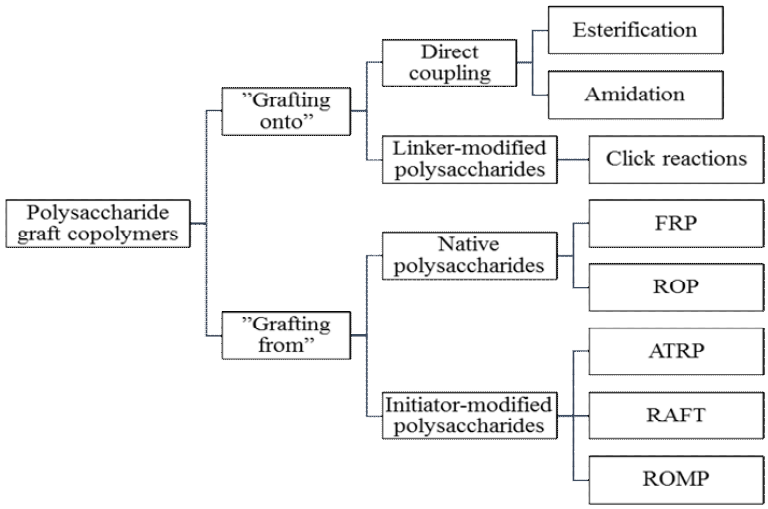

Figure 2 *Synthesis of polysaccharide graft copolymers. FRP - free radical polymerization, ROP - ring-opening polymerization, ATRP - atom-transfer radical polymerization, RAFT - reversible addition-fragmentation chain-transfer polymerization, ROMP - ring-opening metathesis polymerization.*

In the present thesis, water-soluble, high molecular weight polysaccharide graft copolymers with cleavable arms are introduced as drug delivery vehicles for the treatment of eye diseases. These vehicles are designed to undergo a two-stage release specifically tailored to the requirements of back of the eye drug delivery (Figure 3). First, synthetic multifunctional polymer grafts, carrying drugs and targeting ligands, are released from the polysaccharide backbone upon exposure to a first trigger. Second, release of drugs from the grafts takes place after target-mediated cell uptake, which initiates a second trigger. The release mechanism relies on carefully coordinated chemical linkages between copolymer backbone and side chains, as well as between side chains and drugs. While the drug-conjugation has to remain intact in the extracellular environment inside the eye, the linkages between side chains and backbone need to be slowly cleaved.

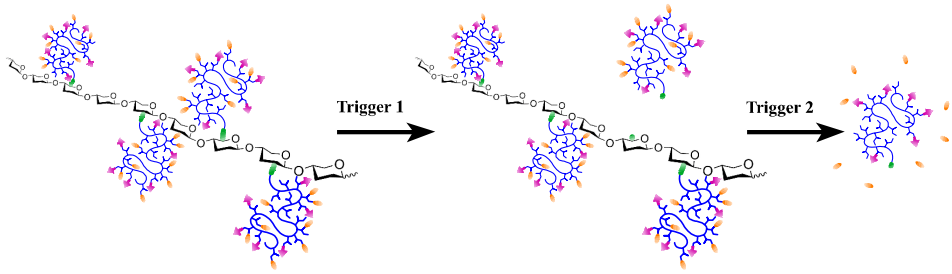

Figure 3 *Two-stage release from polysaccharide graft copolymers: 1) Sustained release of drug- and targeting moiety-carrying grafts upon exposure to first trigger. 2) Release of drugs from the grafts at the site of action initiated by the second trigger.*

1.1.2 Hydrolytically cleavable bonds

Different chemical bonds are used to attach drugs and ligands to polymers and they have varying stabilities in physiological conditions. Bonds can be cleaved by either enzymatic or non-enzymatic hydrolysis.[28] The hydrolytic stability at neutral pH increases from esters < carbonates < carbamates (urethanes) < hydrazones < amides (Scheme 1).[28] Furthermore, hydrazones and acetals are rather stable at neutral pH, but undergo hydrolysis under mildly acidic conditions (*i.e.* pH 5.0) after uptake into the endosomes and lysosomes of cells.[29,30] Peptide linkers are stable in serum, but are readily cleaved by intracellular enzymes, and disulfide linkages are reduced by glutathione over-expressed in tumor cells.[31] The rate of hydrolysis of polymer-drug conjugates is influenced by the type of bonds, hydrophilicity of neighboring groups and steric crowding at the reaction center. Hydrophobic neighboring groups slow down the hydrolysis rate.[32,33] In contrast, use of a spacer between the drug and the polymer backbone decreases the steric hindrance and thus increases the release rate significantly.[34]

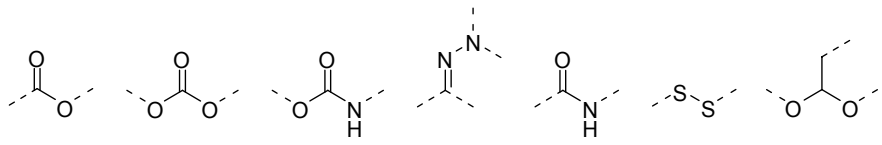

Scheme 1 *Structure of different chemical linkages.*

The copolymer in this work is based on hyaluronic acid (HA), a naturally occurring polysaccharide and constituent of the vitreous, and multihydroxyfunctional poly(glyceryl glycerol) (PGG) side chains. Release of PGG grafts has to occur in the neutral aqueous environment of the vitreous body, *i.e.* the clear gel inside the eye filling the space between lens and retina. This can be achieved by non-enzymatic hydrolysis of ester bonds or by degradation of the hyaluronic acid backbone in presence of hyaluronan-digesting enzymes (hyaluronidases).[35] Hence linkers between HA and the grafts can be ester-based or non-degradable, *e.g.* amides. The attachment of drugs to the polymer grafts can be realized through hydrazone bonds, which are stable at neutral pH and readily cleaved after cell uptake. Targeting ligands and probes will be irreversibly linked to the grafts using amide and thiourea bonds.

1.2 Drug delivery to the back of the eye

1.2.1 Posterior segment ocular diseases

Posterior segment ocular diseases are the leading cause of visual impairment and blindness in the Western societies and their prevalence is expected to increase in future with the proportion of elderly people.[36–38] Diseases, such as age-related macular degeneration (AMD), diabetic retinopathy and macular edema, affect the tissues of the retina and choroid (Figure 5). They are caused by extensive neovascularization and leaky blood vessels of the choroid, which leads to inflammation and damage in retinal cells.[39] Dysfunction of the retinal pigment epithelium (RPE) due to oxidative stress or inflammation is the primary event that leads to deterioration of vision in AMD.[40,41] RPE cells are essential for proper visual function as they provide nutrients and protection for the photoreceptors, and serve as the waste disposal system of the retina. Therefore they are recognized as a target site for the treatment of retinal diseases.[42]

AMD and diabetic retinopathy often require therapy over several years and can be managed with anti-angiogenic drugs that inhibit the growth of new blood vessels. Currently explored therapeutics include corticosteroids (*e.g.* dexamethasone, triamcinolone acetonide) and biologics, such as recombinant fusion proteins (aflibercept), Fab-fragments (ranibizumab) or monoclonal antibodies (bevacizumab) (Figure 4).[36,39,43]

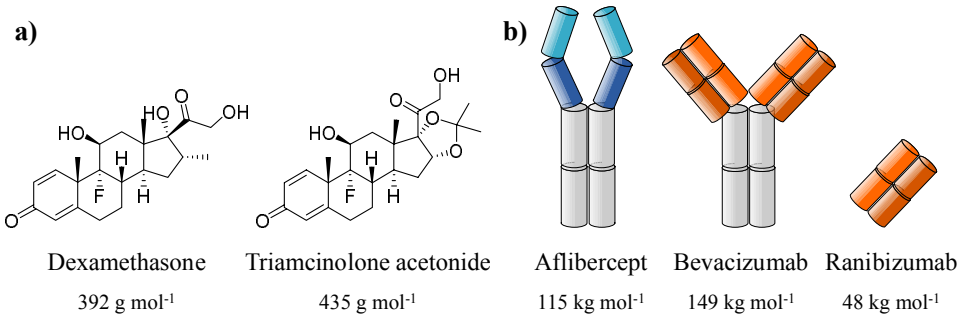

Figure 4 *Structures of corticosteroids (a) and biologic therapeutics (b) used in treatment of posterior segment ocular diseases.*[44]

1.2.2 Physiology and barriers of the eye

The eye features several barriers that effectively hinder drug transport from topically applied formulations (*e.g.* eye drops) and systemic administrations to the vitreous (Figure 5).[45] Intravitreal injections yield the highest retinal drug bioavailability, but frequent injections can increase the probability of complications, such as ocular inflammation, retinal detachment, hemorrhage or endophthalmitis.[46–48] Repeated injections are required due to the short half-life of drugs in the eye.[49]

Clearance of drugs from the vitreous takes place via two pathways (Figure 5, blue arrows). Small molecular weight hydrophobic drugs readily permeate across the blood-retinal barrier and enter systemic blood circulation via the posterior route. This pathway is impeded for larger hydrophilic molecules, which have limited permeability in the RPE.[50] Furthermore, drugs are eliminated via the anterior route by constant vitreous outflow into the anterior chamber with a rate of clearance depending on the diffusivity of the drug.[51] As a result of their low diffusivity and hindered permeation across the RPE, hydrophilic macromolecules exhibit extended residence times in the vitreous.[52,53]

The vitreous humor consists of a highly hydrated network of negatively charged HA with hydrophobic domains of collagen and a mesh size of about 500 nm.[51,54] Hence, neutral or negatively charged molecules and particles of up to 500 nm have similar mobility as in water, while positively charged molecules and larger particles aggregate with the vitreous components.[55] Furthermore, access to the retina and RPE is guarded by inner and external limiting membranes (ILM and ELM) that prevent passage of macromolecules bigger than 10 nm.[50,56] An ideal drug carrier is thus large enough to show prolonged residence time in the vitreous, but also has a way to penetrate the retinal layers and reach the RPE.

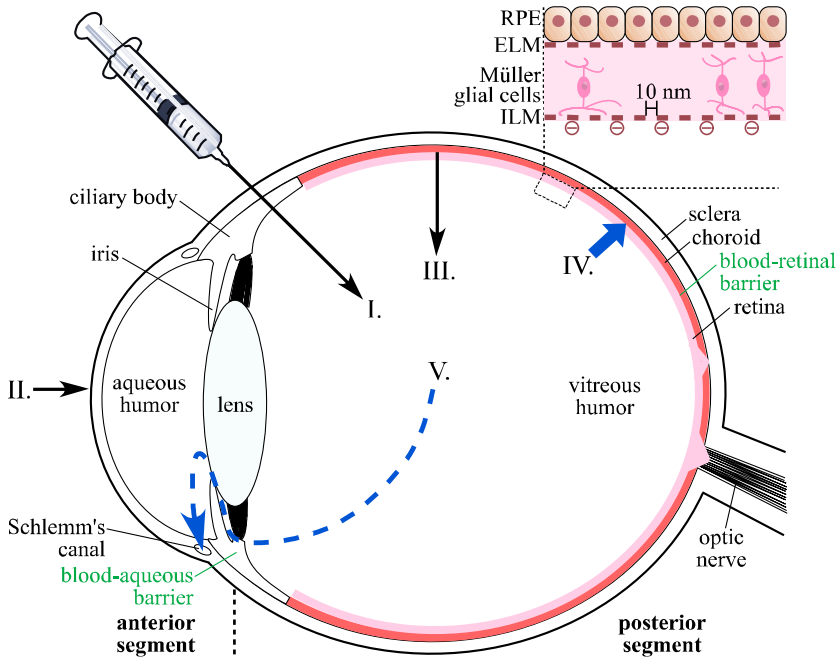

Figure 5 *Structure of the eye with routes of drug administration (I-III) and clearance (IV-V) illustrated, redrawn from reference 45 and article III. Selected methods of administration: I) intravitreal injection, II) topical application, III) drug diffusion across the blood-retinal barrier after systemic application. Clearance pathways: IV) drug elimination via posterior route across blood-retinal barrier, V) diffusion of drugs into anterior chamber and clearance by aqueous humor turnover (anterior route).*

1.2.3 Drug delivery approaches

In recent years many polymeric drug delivery vehicles were proposed to reduce the frequency of required intravitreal injections and to deliver drugs at controlled levels for prolonged times. These include micro- and nanoparticles, dendrimers, hydrogels and polymer implants.[43,57–59] Ozurdex® is a biodegradable polymer implant consisting of a poly(lactide-*co*-glycolide) matrix loaded with dexamethasone.[60,61] Ozurdex® enables controlled drug delivery over months or years, but its implantation is more invasive than standard intravitreal injections. Implants have further been shown to increase the intraocular pressure and the progression of cataract.[62] In contrast, drug-loaded polymer micro- or nanoparticles can be injected. Their distribution in the vitreous greatly depends on their size and surface charge. Nanoparticles have lower settling velocities in the vitreous than microparticles, which leads to longer retention times.[63] However the high surface to volume ratio often results in burst drug release from the nanoparticles.[64] Particle formulations can lead to visual disturbances and aggregates may activate macrophages.[65,66]

Nanoparticle carriers were modified with different targeting ligands to enhance their uptake by RPE cells. Recognition was achieved with biologics, such as arginyl-glycyl-aspartic acid (RGD)-peptides and transferrin,[67] cell penetrating peptides,[42] or nanoparticles made of human serum albumin.[68] Furthermore, folic acid[69,70] and HA[56,71] were shown to induce receptor-mediated endocytosis in RPE cells.

The proposed water-soluble HA-PGG graft copolymer presents a novel approach to intravitreal drug delivery. The vehicle is designed to minimize visual disturbances by being dissolved and to provide long retention time in the vitreous through its high molecular weight. Slow cleavage of grafts from the backbone allows for sustained release of polymer fragments that are small enough to penetrate into retinal layers, but large enough to exhibit significant vitreal half-lives. The multifunctional PGG can carry a variety of drugs, probes and targeting ligands.

1.3 Hyaluronic acid

HA is a linear polysaccharide consisting of disaccharide repeating units of β(1,4)- and β(1,3)-linked D-glucuronic acid and *N*-acetyl glucosamine (Scheme 2). It is present in the extracellular matrix of vertebrates and plays a role in cell proliferation, differentiation and tissue repair.[72] For this study it was selected for its high molecular weight and biocompatibility as a natural constituent of the vitreous. Chemical modification of HA can be achieved in different ways as summarized by Schanté and colleagues.[73] Shortly, the glucuronic acid is commonly esterified, amidated or oxidized, while the primary hydroxyl group of *N*-acetyl glucosamine can be targeted for ether, ester, or carbamate formation. The reducing end of the polysaccharide is often used in reductive amination to yield block copolymers.[74]

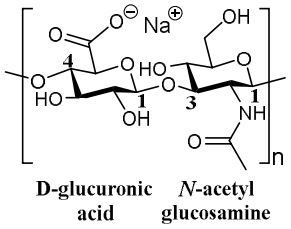

Scheme 2 *Chemical structure of sodium hyaluronate.*

1.3.1 HA (bio)degradation

Chemical modification of HA is subject to two major limitations. The first problem is the pronounced degradation of the polymer under harsh reaction conditions. To preserve the high molar mass of HA, strongly alkaline, acidic or oxidative solutions, heat, shear and microwave irradiation should be avoided.[75,76] The second constraint is the solubility of

sodium hyaluronate (the prevalent form of HA), which is limited to aqueous solutions. Under these conditions, many of the aforementioned reactions proceed with low efficiency and require excess of reagents. Hence, these reactions are unsuitable for direct grafting of HA with elaborately prepared drug- and ligand-carrying polymeric side chains. Exchange of the sodium counter ion for tetraalkylammonium ions or acidification of HA helps to solubilize the polymer in dimethyl sulfoxide (DMSO),[77,78] but these treatments lead to further degradation and complicate the purification of the products.[79,80] Small and reactive linkers, introduced under mild aqueous reaction conditions, can facilitate the grafting of polymer side chains.

Another aspect of HA modification is its impact on the biodegradation behavior. Masking of the D-glucuronic acid moieties of HA inhibits its recognition by hyaluronidase and slows down its degradation in the body.[81,82] Hyaluronidase is present in the human vitreous,[35] therefore functionalization of the D-glucuronic acids possibly prolongs the already long residence time of HA in the eye (half-life of 500 kg mol^{-1} HA in rabbit vitreous is 30 days).[83]

1.3.2 Introduction of reactive linkers onto HA

As mentioned above, polysaccharide graft copolymers with cleavable arms may comprise hydrolytically labile ester or stable amide bonds between the backbone and side chains, depending on the mode of cleavage (*i.e.* hydrolysis of the linker or enzymatic degradation of the backbone). In addition, the linkers must be accessible for efficient coupling of polymers, resulting in the choice of *clickable* linkers. Click chemistry, a term coined by Sharpless and colleagues in 2001,[84] refers to reactions that are chemoselective, high yielding, and devoid of offensive byproducts. They include the widely used copper-mediated azide-alkyne cycloaddition (CuAAC or just click reaction), strain-promoted azide-alkyne cycloaddition, Diels-Alder cycloaddition, thiol-ene conjugation, and recently triazolinedione-based reactions with (di)enes.[85]

Amidation of HA with clickable linkers is commonly achieved by carbodiimide-mediated coupling.[86–88] 1-Ethyl-3-(3-dimethylaminopropyl)carbodiimide (EDC) is a water-soluble coupling agent used to activate carboxyl groups by formation of an *O*-acylisourea intermediate (Scheme 3).[89] The intermediate is highly unstable in aqueous solution and rearranges into an unreactive *N*-acyl urea byproduct, which is covalently bound to HA. Addition of *N*-hydroxysuccinimide (NHS) or 1-hydroxybenzotriazole (HOBt) can stabilize the amine-reactive intermediate by converting it into an active ester.[90] However the method typically produces low degrees of substitution (DS) and requires accurate control of pH (reactivity of EDC is highest at acidic pH, while amines are reactive at neutral or alkaline pH), which is most inconvenient. Triazine-based coupling agents, such as 4-(4,6-dimethoxy-1,3,5-triazin-2-yl)-4-methylmorpholinium chloride (DMT-MM), yield higher DS than EDC/NHS, while demanding no specific pH control and using reduced quantities of coupling agent.[91,92]

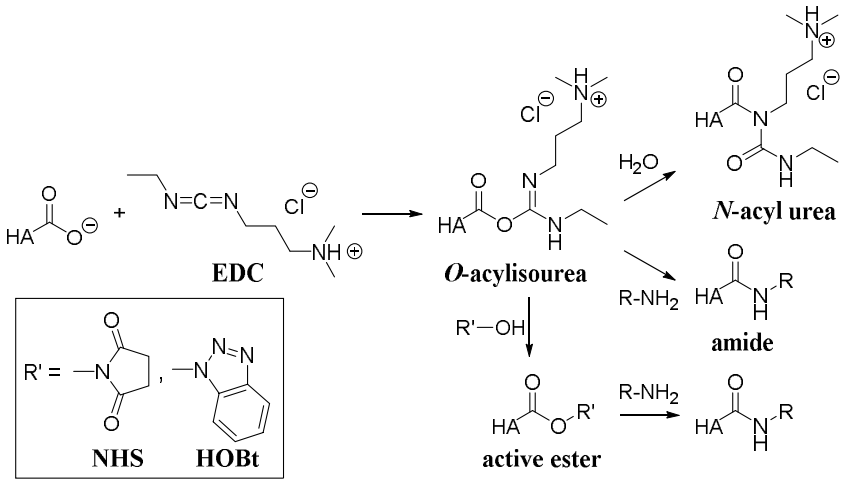

Scheme 3 *Carbodiimide-mediated amidation of HA. Reactive O-acylisourea intermediate rearranges in water to N-acyl urea byproduct or reacts with amine to form the desired amide (competing reactions). The intermediate can be stabilized with NHS or HOBt as active ester, retaining its amine-reactivity.*

Table 1 *Literature procedures for esterification of the HA glucuronic acid groups.*

#	HA[a]	Activator[b]	Reagent	Solvent[c]	DS / %	Ref.
1	Na salt	TEA	Glycidyl methacrylate	PBS / DMF (1:0 to 1:1 v/v)	14-90	93
2	Na salt	DCC / DMAP	Curcumin	H_2O / DMSO (1:1 v/v)	1.4	94
3	Free acid	Diazomethane	Trimethylsilyl diazomethane	DMSO	80-100	95
4	Free acid	DCC / DMAP	Paclitaxel	DMSO	5	78
5	TBA salt	Alkyl halide	Dodecyl / Octadecyl bromide	DMSO	1-5	96
6	TBA salt	Tosylate or alkyl halide	Tetraethylene glycol ditosylate / dodecyl bromide	DMSO	0.5-4.7	77
7	TBA salt	Alkyl halide	Alkyl iodide (n = 1-6)	DMSO	50-100	97

[a]Form of hyaluronic acid employed in reactions (TBA - tetrabutylammonium). [b]DCC - *N,N'*-dicyclohexylcarbodiimide, DMAP - 4-dimethylaminopyridine, TEA - triethylamine. [c]DMF - dimethylformamide, PBS - phosphate-buffered saline.

Esterification of the glucuronic acid groups of HA is usually accomplished in two steps. First the polysaccharide is converted into its acidic form or quaternary ammonium salt; then it is dissolved in an aprotic solvent and reacted with an esterifying agent (Table 1). HA derivatives with high DS are often insoluble in water.[10] Ethyl and benzyl esters of HA, termed HYAFF® 7 and HYAFF® 11, are widely studied as membranes, fibers, sponges, and microspheres for biomedical applications.[98] A few studies report the esterification of sodium hyaluronate in aqueous solvent mixtures (Table 1, entries 1&2),

but yield very low DS or use tremendous excess of reagents (*i.e.* 50-100-fold molar excess of glycidyl methacrylate compared to carboxyls). To minimize the degradation of the polysaccharide backbone, esterification of *untreated* HA with clickable linkers is one topic of this work.

1.3.3 HA in ophthalmology

HA has been employed in ophthalmic viscosurgery since the early 1980s.[99] Used in the form of highly viscoelastic solutions, it serves as vitreous replacement after vitreoretinal surgery, for tissue protection during corneal transplantation or as topical formulation to hydrate the surface of the eye. Lai *et al.* reported cross-linked HA hydrogel discs as cell sheet delivery systems for corneal epithelial cells.[100] After implantation of the discs into the anterior chamber of rabbit eyes, they noticed a marked difference in biocompatibility between glutaraldehyde- and EDC-cross-linked gels. The latter were tolerated much better, provoking no inflammation, and demonstrating the influence of coupling agent on the biocompatibility. Furthermore, UV-curable hydrogels, consisting of thiol-modified HA and alkene-modified PAMAM dendrimers, were investigated as drug delivery systems for the treatment of corneal inflammation.[101] Injected between the conjunctiva and sclera, the gels contained free dexamethasone-carrying dendrimers that were slowly released from the depot and able to target activated corneal macrophages.

For posterior segment diseases, HA is used as a coating material for different types of nanocarriers. Gan *et al.* first demonstrated the targeting ability of HA toward RPE cells.[56] They prepared core-shell nanoparticles made of chitosan and coated with 1,2-dioleoyl-*sn*-glycero-3-phosphoethanolamine (DOPE) lipids. They covalently attached HA to the amine groups of DOPE. In cell uptake studies they found that particles of 200-300 nm size were unable to penetrate the retinal layers of normal rat eyes. The particles only entered the retina of animals with experimentally induced uveitis, a form of ocular inflammation. In this case, HA-coated particles showed enhanced uptake by RPE cells due to their interaction with expressed CD44-receptors. This study illustrates the importance of the size of potential drug carriers, which need to pass the barriers of the inner and external limiting membranes to reach their target site. Martens *et al.* functionalized gene carriers with HA to improve their mobility in the vitreous and enhance their transfection efficiency in RPE cells compared to poly(ethylene glycol) coated vectors.[71] They further found that lipoplexes with a covalently bound HA-shell exhibit 8-fold increased transgene expression compared with uncoated lipoplexes or lipoplexes with electrostatically-bound HA.[102]

A soluble ocular drug delivery vehicle based on HA is yet unprecedented. Due to the high molecular weight of the proposed HA-PGG graft copolymer, the targeting ability of HA will be secondary. The copolymer will be unable to penetrate into the retinal layers as such, considering the radius of gyration of a ~900 kg mol^{-1} HA is approximately 100 nm.[10,103] Rather, smaller fragments, which are released by hydrolytic cleavage of the side chains or degradation of the HA backbone, will facilitate the site specific drug delivery to the RPE. Hence, it is important for the grafts to be multifunctional and display additional targeting ligands to interact with RPE after they are cleaved from HA.

1.4 Multifunctional linear polyethers

Poly(ethylene glycol) (PEG) is the most frequently used water-soluble polymer in biomedical applications. It is attached to proteins, drugs, liposomes, and polymer particles (PEGylation) to enhance their solubility and circulation time *in vivo*. The so-called stealth effect is attributed to PEG's highly hydrated and flexible structure, which shields the conjugates from protein adsorption, thereby preventing recognition by the immune system.[104] PEG-drug conjugates exhibit intrinsically low payloads, because the linear polyether has only two functional groups for derivatization.[105] Furthermore, formation of anti-PEG antibodies was observed, causing hypersensitivity and enhanced blood clearance after repeated injections.[106] The concerns about the safety of PEG and its low functionality have thus led to the search of other hydrophilic polymers as substitutes.[107]

In recent years, linear polyglycerols (PGs) have emerged as multifunctional PEG alternatives.[108,109] PG features a PEG backbone with pendant hydroxyl groups in every repeating unit that can be conjugated with a variety of drugs, probes and targeting ligands (Scheme 4). Poly(glyceryl glycerol) (PGG), which is in the focus of this study, is a linear PG with pendant glycerol moieties, offering additional options for functionalization while maintaining a compact size. PGs are highly hydrophilic, possess excellent antifouling properties and superior biocompatibility compared with PEG, as they are showing neither activation of the complement system nor red blood cell aggregation or hemolysis.[110–112] Linear polyglycerols are prepared by oxyanionic ring-opening polymerization (ROP) of protected glycidol derivatives (glycidyl ethers).

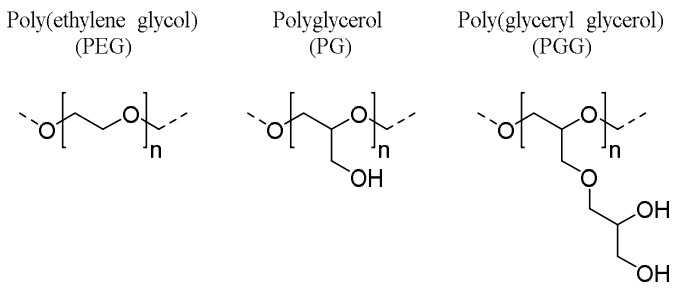

Scheme 4 *Structures of poly(ethylene glycol), polyglycerol and poly(glyceryl glycerol); the latter is in the focus of this study.*

1.4.1 Ring-opening polymerization of epoxides

Epoxide monomers can be polymerized by anionic or cationic ring-opening polymerization (AROP and CROP), but AROP is more efficient in achieving well controlled molecular weight, dispersity and end group functionality.[113] Any pendant hydroxyl groups of the monomers must be protected during polymerization, otherwise hyperbranched polyethers are obtained. Acetal protecting groups are commonly used and afterwards removed under acidic conditions. The polymerization mechanism (Scheme 5) involves the bimolecular nucleophilic substitution of an initiator on the epoxide ring,

leading to an alkoxide growing chain, which attacks another monomer. The reaction is terminated by proton transfer from an acidic compound (often water or alcohols), resulting in a hydroxyl end group.

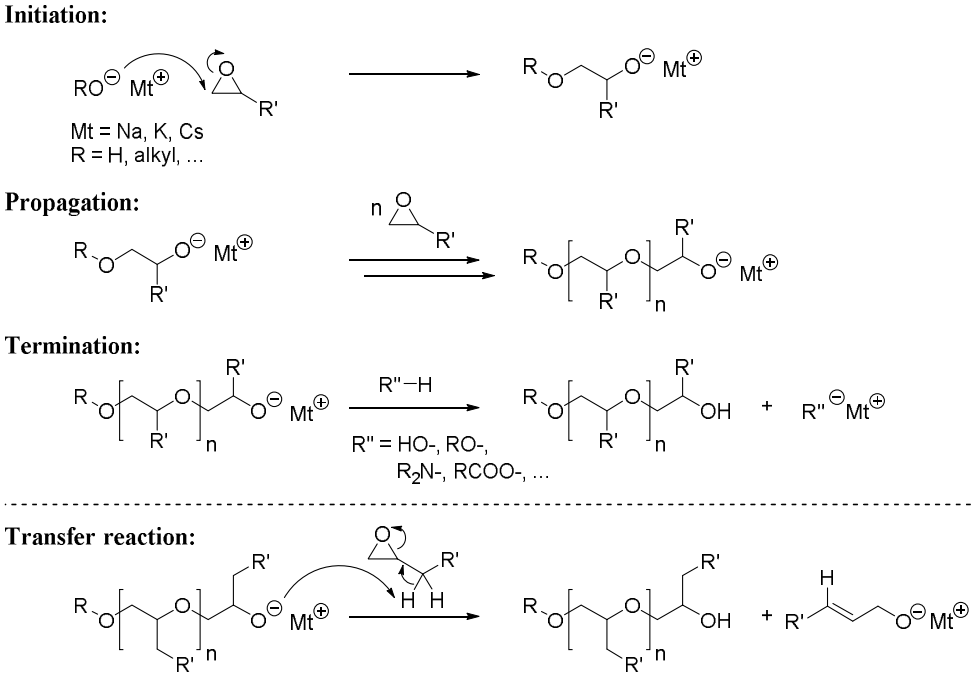

Scheme 5 *Mechanism of anionic ring-opening polymerization of epoxide monomers initiated by alkali metal alkoxides (initiation, propagation, termination).[113] In case of mono-substituted epoxides, transfer reactions occur in presence of strongly basic alkali metal alkoxides.*

Alkali metal alkoxides were used to initiate AROP of ethylene oxide and several glycidyl ether monomers,[114,115] but they are strongly basic and abstract protons from mono-substituted epoxides leading to transfer reactions (Scheme 5). Transfer reactions strongly limit the molecular weight that can be obtained for polyethers and are more pronounced at higher temperatures.[116] Polymerization temperatures can be effectively reduced with the help of larger counter ions. For example, use of cesium instead of sodium or complexation of the counter ion with crown ethers results in decreased aggregation with the chain end and thus higher reactivity. In this way, side reactions can be suppressed.

Another approach to increase the polymerization rate was developed by Carlotti, Deffieux *et al.* using Lewis acidic trialkylaluminum as a monomer activator.[117,118] The aluminum compound forms a complex with the epoxide oxygen, thereby enhancing the reactivity of the ring α-carbon toward nucleophilic attack. For monomer activation, an excess of the Lewis acid compared to the initiator is required, as both form a 1:1 complex together. A further development was the substitution of alkali metal alkoxides with

ammonium salt initiators leading to higher molecular weights and even faster polymerization kinetics.[119] In these systems transfer reactions are greatly suppressed due to the decrease in chain end basicity by coordination to aluminum.

1.4.2 Post-polymerization modification of poly(glyceryl glycerol)

Heterofunctional polyglycerols, *i.e.* polymers with different head-, end- and side-groups, can be obtained in various ways. Use of functional initiators that tolerate the harsh polymerization conditions leads to α-functional polyethers. For example, protected amine and thiol head groups, as well as catechol, adamantyl, and cholesterol groups have been introduced.[109] Deffieux's monomer-activated polymerization method allows for the direct preparation of α-bromo- and α-azido-polyethers; the latter are useful in click reactions.[120] End group modification can be achieved by capping of the "living" chain end with alkyl halides and anhydrides or functionalization of the protected polymers' ω-hydroxyl group by esterification or ether synthesis. This approach was used in the synthesis of propargyl-terminated PGs and for preparation of methacrylate- and styrene-capped polyglycerol macromonomers for radical polymerization.[121,122]

Chemical modification of the pendant hydroxyl groups in deprotected polyglycerol has been achieved by esterification in dimethylformamide (DMF) with *e.g.* acetic anhydride,[123] palmitoyl chloride,[124] and 3,3-dithiopropionic acid.[125] Li and Chau published a comprehensive study detailing the synthesis of 18 monofunctional and 9 heterobifunctional derivatives of poly(glycerol-*co*-ethylene oxide) random copolymers, performing most of the reactions in either tetrahydrofuran or dichloromethane.[126] The authors noted that copolymers with monomer ratios of ethylene oxide/glycidol < 19:1 were insoluble in nonpolar solvents. The limited solubility of PG, and especially PGG, in common organic solvents is a major drawback compared with PEG. Hence, it is subject of the present work to develop strategies for efficient conjugation of PGG with functional moieties, such as drugs, probes and targeting ligands.

2 Objectives of the study

This study was aimed at synthesizing a water-soluble and biocompatible hyaluronic acid-based graft copolymer with cleavable arms as a vehicle for intravitreal drug delivery. The copolymer should exhibit high molecular weight to prolong its retention within the vitreous and be able to slowly release its grafted side chains. The side chains should be multifunctional and facilitate the attachment of various bioactive molecules, such as drugs, targeting ligands and probes.

In this work:

(i) Methods were developed to modify hyaluronic acid (HA) with reactive groups for efficient grafting of side chains.[I,III] The influence of reaction conditions on molecular weight of HA was studied and procedures were optimized to reduce polysaccharide degradation and to achieve efficient modification.

(ii) Multifunctional polyether grafts were synthesized by monomer-activated ring-opening polymerization of epoxides.[II] Coupling of the pendant hydroxyl groups with various probes was investigated.[II,III] Conversion of hydroxyls into reactive hydrazides for further attachment of drugs and targeting ligands was accomplished.

(iii) Polyether chains were grafted onto HA-derivatives via copper-mediated azide-alkyne cycloaddition.[III] Polymer-from-polymer release of grafts from the polysaccharide backbone was studied under simulated vitreal conditions.[III] Different experimental setups were explored to quantify release rates. Release kinetics of polymer side chains were compared with release of small molecules from HA.

(iv) Biocompatibility studies were performed with the synthesized materials in cell cultures.[III]

3 Experimental

This section briefly describes the synthetic and analytical procedures used in this study. Detailed instructions can be found from the respective publications.

3.1 Characterization

The structures of all small molecules, polymers and polymer-derivatives were confirmed by nuclear magnetic resonance spectroscopy (NMR) using a Bruker Avance III 500 spectrometer (^{1}H: 500.13 MHz, ^{13}C: 125.77 MHz). Boronic ester formation between PGG 1,2-diol groups and phenylboronic acid was investigated by diffusion-ordered NMR (DOSY) using the standard Bruker pulse sequence *ledbpgp2s*. The hydrolysis of HA-propargyl ester (c = 1 mg mL^{-1}) to release propargyl alcohol was studied in PBS (pH 7.40) containing 5 % (v/v) deuterium oxide (D_2O) at 37 °C. ^{1}H NMR spectra were acquired using a water presaturation pulse (*zgpr*, pulse strength 1 mW) to partially suppress the solvent signal.

Molecular weights and distributions of HA(-derivatives) and PGG were determined by size exclusion chromatography (SEC) in 0.1 M aqueous sodium nitrate ($NaNO_3$) solution containing 3 % (v/v) acetonitrile. Samples were eluted at 0.8 mL min^{-1} using a Waters 515 HPLC pump and Waters 2410 refractive index detector. The column set comprised a TOSOH guard column PWXL and TSKgel columns G3000 PWXL, G5000 PWXL, and G6000 PWXL. Chromatograms were calibrated with narrow poly(ethylene oxide) standards (PSS Polymer Standards Service), unless otherwise noted. Protected polyethers (PIGG) were measured with the same equipment using Waters Styragel guard column and Styragel HR1, HR2, and HR4 columns. PIGG was eluted with tetrahydrofuran containing 1 % (v/v) toluene and calibrated with narrow polystyrene standards (Scientific Polymer Products, Inc.).

Fourier transform infrared (FT-IR) spectra were recorded using a Perkin Elmer One FT-IR spectrometer with attenuated total reflection accessory. Fluorescence measurements were performed with a Horiba Jobin Yvon FluoroMax-4 spectrofluorometer. Ultraviolet (UV) spectra were measured using a Shimadzu UV-1601PC UV-visible spectrophotometer.

3.2 Syntheses

3.2.1 Functionalization of HA[I,III]

High molecular weight HA (~750 kg mol^{-1} according to manufacturer) was used in all syntheses. The products were typically purified by aqueous dialysis and lyophilized.

Gravimetric yields were generally around 80 %. Degrees of substitution (DS) were determined by ^{1}H NMR and are given in percent per 100 disaccharide repeating units.

Triazine-mediated amidation of HA was performed according to the procedure of Bergman *et al.*[91] The coupling agent (DMT-MM) was generated in situ from 2-chloro-4,6-dimethoxy-1,3,5-triazine (1.0 eq.) and *N*-methylmorpholine (1.5 eq.) in water/acetonitrile (3:2 v/v). Functional amines were employed at a 1.5-molar excess compared to the HA carboxyl groups. NMR kinetic studies were performed in unbuffered D_2O with low molecular weight HA (~1 kg mol^{-1}) and DMT-MM prepared *ex situ*.[127]

The esterification method was inspired by the work of Nishikubo *et al.*, who reacted poly(methacrylic acid) with alkyl halides in the presence of bases in aqueous mixtures.[128] The reaction conditions were optimized to be suitable for the modification of HA with propargyl derivatives (Table 2). HA was first dissolved in water; DMSO was added dropwise under cooling on ice, followed by addition of other reagents.

Table 2 *Excerpt of esterification conditions tested for the preparation of HA-propargyl esters.*[III]

	RX[a]	Base[b]	[HA]:[RX]:[Base]	[HA] / g L^{-1}	H_2O/DMSO (v/v)	T / °C	t / h	DS / %	M_n[c] / %
1	Br	TEA	1.0 : 1.0 : 1.0	2.6	1 : 3	45	24	40	n.d.
2	Mes	TEA	1.0 : 1.0 : 1.0	2.5	1 : 3	45	24	30	55
3	Mes	TEA	1.0 : 3.0 : 3.0	2.5	1 : 3	60	20	26	30
4	Mes	TEA	1.0 : 1.0 : 1.0	2.0	7 : 3	30	48	0	50
5	Br	DBU	1.0 : 2.0 : 2.0	5.0	1 : 3	30	96	0	26
6	Br	DBU	1.0 : 5.0 : 5.0	5.0	1 : 3	30	96	23	17

[a]Substrate in base-catalyzed esterification: propargyl bromide or propargyl mesylate. [b]TEA - triethylamine, DBU - 1,8-diazabicyclo[5.4.0]undec-7-ene. [c]Molecular weight compared to starting weight as determined by SEC.

3.2.2 Ring-opening polymerization of IGG[II]

Reactions were performed under stringent dry conditions in an argon atmosphere. (DL-1,2-Isopropylidene glyceryl) glycidyl ether (IGG), prepared as reported,[129] was polymerized in presence of triisobutylaluminum (Al-*i*Bu$_3$) and an initiator (tetrabutylammonium azide, NBu$_4$N$_3$, or tetraoctylammonium bromide, NOct$_4$Br) in toluene (Table 3). Polymerizations were initiated at -30 °C for 30 min, then continued at room temperature for 24 h, and quenched with methanol. Conversions were typically 100 % as determined by ^{1}H NMR.

Al-*i*Bu$_3$ was removed by precipitation in cold diethyl ether and filtration. The protected polymers (PIGGs) were converted to their azide-derivatives by substitution of the bromide head group with sodium azide, if necessary, and subsequently deprotected in presence of trifluoroacetic acid to yield α-azido-poly(glyceryl glycerol) (N_3-PGG). Gravimetric yields were typically around 80-97 %.

Table 3 *Polymerization conditions and characteristics of polymers before (PIGG) and after deprotection (PGG).*

Polymer	[IGG] / M	Initiator	[Al-*i*Bu$_3$]/[I]	DP$_{theor.}$	M$_{n,theor.}$[a] / kg mol^{-1}	M$_{n,SEC}$[b] / kg mol^{-1}	PDI$_{SEC}$[b]
PIGG-1	3.0	NBu_4N_3	4.0	40	7.5	7.4	1.29
PGG-1	-	-	-	40	5.9	3.5	1.49
PIGG-2	2.0	NBu_4N_3	5.0	40	7.5	5.1	1.27
PGG-2	-	-	-	40	5.9	2.3	1.53
PIGG-3	2.0	NBu_4N_3	5.0	20	3.8	6.6	1.39
PGG-3	-	-	-	20	3.0	3.1	1.62
PIGG-4	3.0	$NOct_4Br$	4.0	67	12.6	13.9	1.60
PGG-4	-	-	-	67	9.9	9.2	1.45
PIGG-5	3.0	$NOct_4Br$	4.0	67	12.6	11.1	1.13
PGG-5	-	-	-	67	9.9	5.8	1.21
PIGG-6	3.0	$NOct_4Br$	4.0	51	9.6	9.1	1.36
PGG-6	-	-	-	51	7.6	3.5	1.25

[a]Theoretical molecular weight calculated from the molar ratio of monomer to initiator. Conversion was 100 % in all polymerizations as determined by ^{1}H NMR. [b]SEC of PIGG in THF calibrated with polystyrene standards; SEC of PGG in 0.1 M $NaNO_3$ calibrated with poly(ethylene oxide) standards.

3.2.3 Functionalization of PGG

3.2.3.1 Pyrene-ether of PGG[III]

PGG-pyrene was prepared by Williamson ether synthesis (Scheme 6). PGG (1.0 eq. hydroxyl groups) was activated with sodium hydride (1.2 eq.) in dry DMF and coupled with 1-bromomethylpyrene (0.1 eq.). The product was purified by precipitation in cold acetone and aqueous dialysis (Gravimetric yield: 63 %). The pyrene content was determined by ^{1}H NMR and UV spectroscopy.

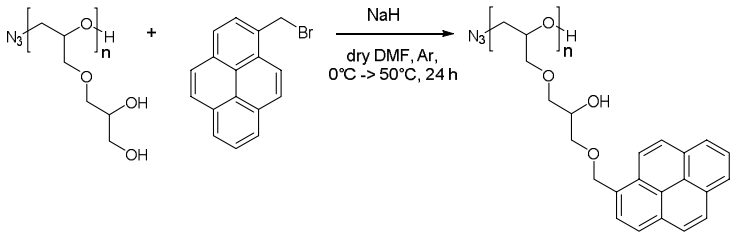

Scheme 6 *Synthesis of PGG-pyrene. Pyrene may be attached to any of the hydroxyl groups.*

3.2.3.2 Rhodamine B-labeling of PGG particles[II]

N_3-PGG (3.5 kg mol^{-1}) was coupled to propargyl-functional poly(L-lactide) (PLLA, 5.9 kg mol^{-1}) by copper-mediated azide-alkyne cycloaddition. The amphiphilic block copolymers were assembled into particles of ~70 nm diameter by nanoprecipitation into phosphate-buffered saline (PBS, pH 7.4). The particles exhibited a hydrophilic PGG-shell.

Particle dispersions were mixed with solutions of either rhodamine B-boronic acid or plain rhodamine B, corresponding to 0.1 equivalent of PGG 1,2-diols. Subsequently, the mixtures were dialyzed against PBS (molecular weight cut-off, MWCO 3.5 kg mol^{-1}) until no more dye was released into the dialysate as monitored by fluorescence spectroscopy. The remaining dye concentration in the dispersions was determined by fluorescence spectroscopy and compared to calibration curves of the individual dyes.

3.2.3.3 Synthesis of PGG-hydrazide

The procedure was inspired by the work of Liu *et al.*,[130] but adapted to be suitable for modification of PGG (Scheme 7). PGG (655 mg, 8.8 mmol hydroxyl groups, 1.0 eq.) was dried in vacuum and dissolved in dry DMF (c = 10 mg mL^{-1}) under argon. The solution was cooled to 0 °C in an ice bath and sodium hydride (NaH, 55 % in mineral oil, 544 mg, 12.5 mmol, 1.4 eq.) was added under argon. The suspension was stirred in the thawing ice bath overnight. Tetrabutylammonium iodide (NBu_4I, 979 mg, 2.7 mmol, 0.3 eq.) was added under argon at room temperature. Methyl bromoacetate (2.68 mL, 28.3 mmol, 3.2 eq.) was added dropwise via syringe. The mixture was placed in an oil bath at 40 °C and stirred for 3 days. The crude mixture was subsequently added to 200 mL water under stirring. The resulting yellow suspension was centrifuged for 10 min at 10 °C and 20 414 x *g*. The pellet was dispersed in water and centrifuged again (3 times) and finally collected with water and lyophilized to give a light beige powdery solid (PGG-acetate, gravimetric yield: 205 mg, 31 %).

Hydrazine hydrate (80 %) was added to PGG-acetate (c = 20 mg mL^{-1}) and the mixture was stirred at 60 °C overnight. The resulting solution was diluted with water, dialyzed (MWCO: 1000 g mol^{-1}) against water for 3 days and lyophilized. Gravimetric yield: 188 mg, 92 % (DS = 33 % of repeating units by ^{1}H NMR).

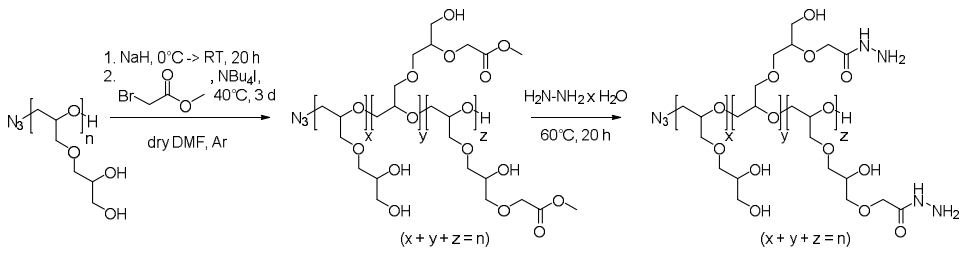

Scheme 7 *Two-step synthesis of PGG-hydrazide: 1. etherification with methyl bromoacetate, 2. hydrazinolysis. (unpublished)*

3.2.4 Copper-mediated azide-alkyne cycloadditions (CuAAC)[III]

The assessment of polysaccharide degradation under CuAAC conditions was performed with HA-propargyl ester and sodium azide (NaN_3) as a model compound.

Method A) To an aqueous solution of HA and NaN_3 was added copper(II) sulfate pentahydrate and sodium ascorbate under argon. The mixture was stirred at room temperature and protected from light for 24 h.

Method B) A solution of HA and NaN_3 in water/DMSO (1:3 v/v) was degassed by freeze-pump-thaw cycles. Copper(I) bromide and *N,N,N',N'',N''*-pentamethyl-diethylenetriamine (PMDETA) were added under argon and the mixture was stirred at room temperature and protected from light for 24 h.

Both products were purified by aqueous dialysis in the presence of ethylenediamine-tetraacetic acid (EDTA) to remove copper ions and lyophilized (Gravimetric yield > 92 %). The products were studied by SEC to determine their molecular weights.

Grafting of N_3-PGG onto HA-propargyl ester was accomplished using method B. Graft copolymers were purified by aqueous dialysis with large MWCO and, when indicated, extracted with methanol.

3.3 Polymer-from-polymer release studies[III]

The release of PGG-pyrene grafts from the HA-PGG ester graft copolymer was studied with two different setups. HA-PGG (c = 1 mg mL^{-1}) was incubated in PBS (pH 7.40) at 37 °C.

3.3.1 SEC study

The incubation solution was distributed into Eppendorf vials (1 mL each), which were placed in an oven at 37 °C. At predetermined intervals, samples were withdrawn and frozen in liquid nitrogen. Samples were lyophilized and stored in a freezer until SEC measurements. Immediately before the measurement, one sample at a time was thawed and quickly mixed with SEC eluent containing 1 mg mL^{-1} uracil as an internal standard. The sample was filtered and injected into the chromatograph. The resulting chromatograms were referenced toward the uracil elution volume, baseline corrected, smoothed, and integrated using OriginPro® 8.6 (OriginLab Corporation).

3.3.2 Dialysis study

Two microdialysis devices were used. Both devices were cylindrical in shape and had a membrane attached to their base (Figure 6). The Slide-A-Lyzer® Mini (Thermo Scientific) had a volume of 100 µL and MWCO of 20 kg mol^{-1}. The QuixSep® micro dialyzer (Membrane Filtration Products) was equipped with a 25 kg mol^{-1} MWCO membrane

(Spectra/Por, Spectrum Labs) and had a volume of 1 mL. Solutions of PGG-pyrene or HA-PGG-pyrene ester copolymer were loaded into the devices and dialyzed against PBS at 37 °C under stirring. At preset times, the whole dialysate was replaced with fresh buffer and the concentration of PGG-pyrene in the dialysate was determined by fluorescence spectroscopy.

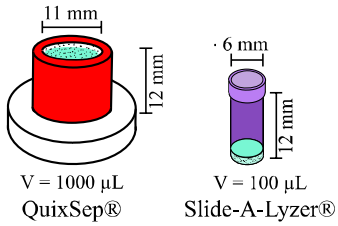

Figure 6 *Dimensions of tested dialysis devices.*

3.4 Biocompatibility[III]

The cytotoxicity of PGG and HA-PGG ester copolymer was evaluated in four different cell lines by means of MTT assay. These included ARPE-19 cells (human retinal pigment epithelial cell line, ATCC CRL-2302), HUVEC (human umbilical vein endothelial cells, ATCC CRL-1730), SKOV-3 (human ovarian adenocarcinoma cells, ATCC HTB-77), and CV-1 (monkey kidney fibroblast cells, ATCC CCL-70).

The cells were seeded in 96 well plates at a density of 20 000 cells per well and incubated in growth medium overnight. After washing, the cells were incubated for 5 h with polymers dissolved in growth medium. Branched poly(ethylene imine) (PEI, 25 kg mol^{-1}) and polyvinyl alcohol (PVA, 30-70 kg mol^{-1}) served as reference compounds. After 5 h the polymer solutions were aspirated, the cells were washed and incubated in growth medium for 24 h. MTT (3-(4,5-dimethylthiazol-2-yl)-2,5-diphenyltetrazolium bromide) solution was added to all wells and incubated for 4 h. Formazan crystals were dissolved with sodium dodecyl sulfate and hydrochloric acid overnight and quantified by UV measurements at 570 nm. Cell viability was calculated as percent compared to untreated cells.

4 Results and Discussion

This section discusses the synthesis and chemical modification of the individual components of the graft copolymer, as well as the properties and release behavior of the HA-PGG conjugate (Figure 7). First, functionalization of the HA backbone is presented, followed by synthesis and post-polymerization modification of PGG side chains. The third part addresses the grafting of PGG onto HA and finally the polymer-from-polymer release is examined including studies of the biocompatibility of the materials.

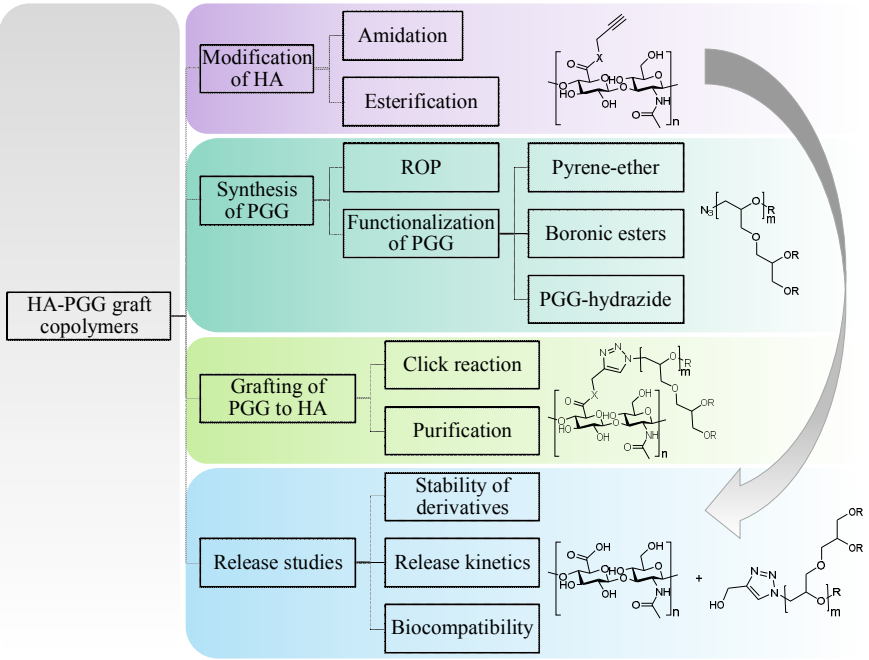

Figure 7 *Schematic representation of the topics covered in the Results and Discussion section.*

4.1 Modification of hyaluronic acid

HA was functionalized with reactive linkers for subsequent grafting of polymer side chains. The glucuronic acid moieties were converted into amides or esters. Ester bonds can be rapidly hydrolyzed in the neutral aqueous environment of the vitreous, while amide bonds are stable.[28] Reactive amide linkers can be used to attach probes to the HA backbone to follow its fate in the vitreous independent of the side chains. Furthermore amide-linked graft copolymers may be degraded by HA-digesting enzymes, resulting in polymer grafts carrying HA fragments (Scheme 8). The chemical modification of HA was investigated with respect to achievable degree of substitution (DS) and minimal polysaccharide degradation.

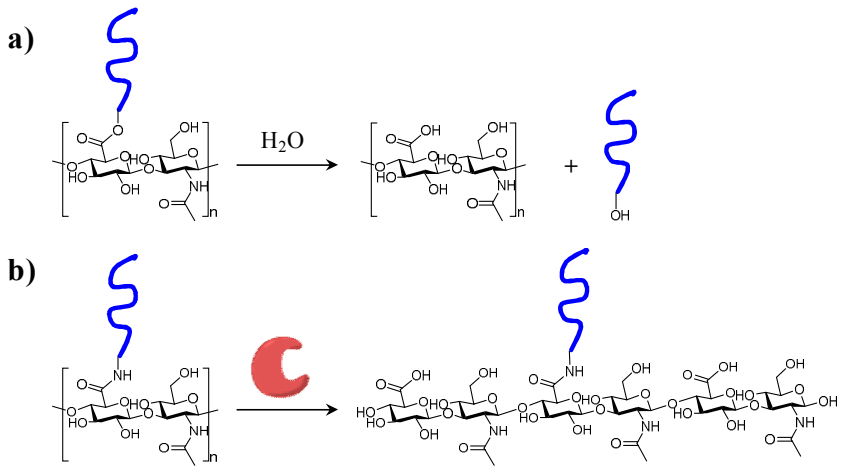

Scheme 8 *Cleavage of side chains from HA graft copolymers with ester or amide linkages. a) Hydrolysis of ester bonds under neutral aqueous conditions. b) Release of grafts carrying HA fragments upon hyaluronidase-mediated degradation of the backbone.*

4.1.1 Triazine-mediated amidation[I]

HA was reacted with several clickable amines using 4-(4,6-dimethoxy-1,3,5-triazin-2-yl)-4-methylmorpholinium chloride (DMT-MM) to activate the glucuronic acid groups. DS of amidated HAs was found to decrease with increasing basicity of the amine reagent (Table 4). The difference in DS was explained in view of the reaction mechanism (Scheme 9). First, the HA-carboxylate attacks DMT-MM to form the "superactive ester" (**AE**). The ester is then attacked by the amine, forming a tetrahedral intermediate (**TI**), and finally collapses to expel a leaving group (**LG**). In case of the "superactive" triazine ester, breakdown of **TI** is energetically favored by the tautomeric rearrangement of **LG**.[131] Therefore the amine attack becomes the rate-limiting process, which is only possible if the amine is not protonated. Conducting the reaction under neutral aqueous conditions resulted in amines with increasing basicity being increasingly protonated and hence inactive.

Table 4 *Degree of substitution of HA amide derivatives prepared from different amines.*[I]

Derivative	Amine reagent	pK_a of amine	DS[a] / %
HA-propargyl	Propargyl amine hydrochloride	8.2	54.5 ± 4.4
HA-maleimide	*N*-(2-Aminoethyl)-maleimide trifluoroacetate	8.4	39.5 ± 2.6
HA-methacrylate	2-Aminoethylmethacrylate hydrochloride	8.8	41.3 ± 6.1
HA-allyl	Allylamine	9.5	28.2 ± 2.2
HA-thiol	Cysteamine hydrochloride	10.8	3.7 ± 0.7

[a]From ^{1}H NMR in D_2O/DMSO-d_6 (1:1 v/v), average of three integrations ± standard deviation.

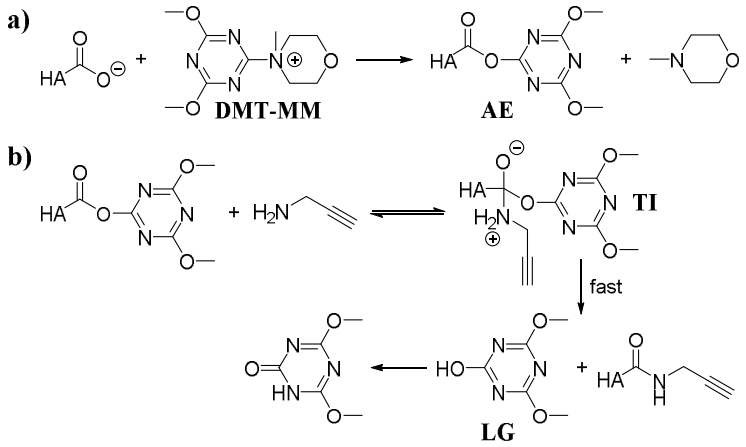

Scheme 9 *Mechanism of triazine-mediated amidation of HA with propargyl amine.*

At the time of this finding, the factors influencing the outcome of triazine-mediated amidations had not been established yet. D'Este *et al.* published a study concurrent to this work, hypothesizing that the reaction rate did not depend on the concentration of the HA-triazine ester.[92] Using ^{1}H NMR spectroscopy, we investigated the kinetics of HA activation and the stability of the coupling agent in aqueous solution. The latter was important as HA coupling reactions are often pursued for several days, but the stability of DMT-MM was only documented for 3 h.[127] The coupling reagent was found to slowly hydrolyze in D_2O ($t_{1/2}$ ~9.2 d). The hydrolysis product, 2-hydroxy-4,6-dimethoxy-1,3,5-triazine (DMT-OH), rearranged to 4,6-dimethoxy-1,3,5-triazin-2-one and subsequently isomerized to a stable isocyanuric acid derivative by *O→N* migration of one methyl group (Scheme 10). Isomerization of DMT-OH was rapid (Figure 8a). In the presence of HA, DMT-MM was consumed faster and the HA-triazine ester, although indistinguishable from DMT-OH by ^{1}H NMR, was formed quantitatively (1.5 eq. of coupling agent was used compared to HA carboxyls) and remained stable for about 10 days in the mixture (Figure 8b).

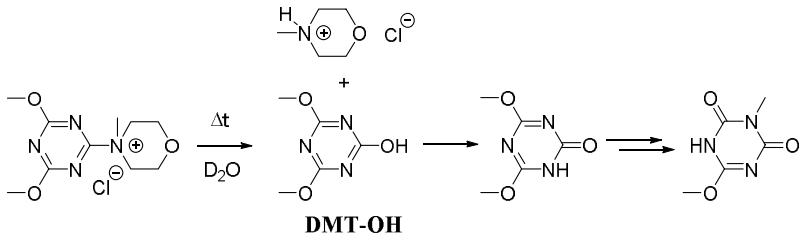

Scheme 10 *Hydrolysis of DMT-MM to DMT-OH and N-morpholinium chloride, followed by rearrangement and isomerization of DMT-OH into the isocyanuric acid derivative.*

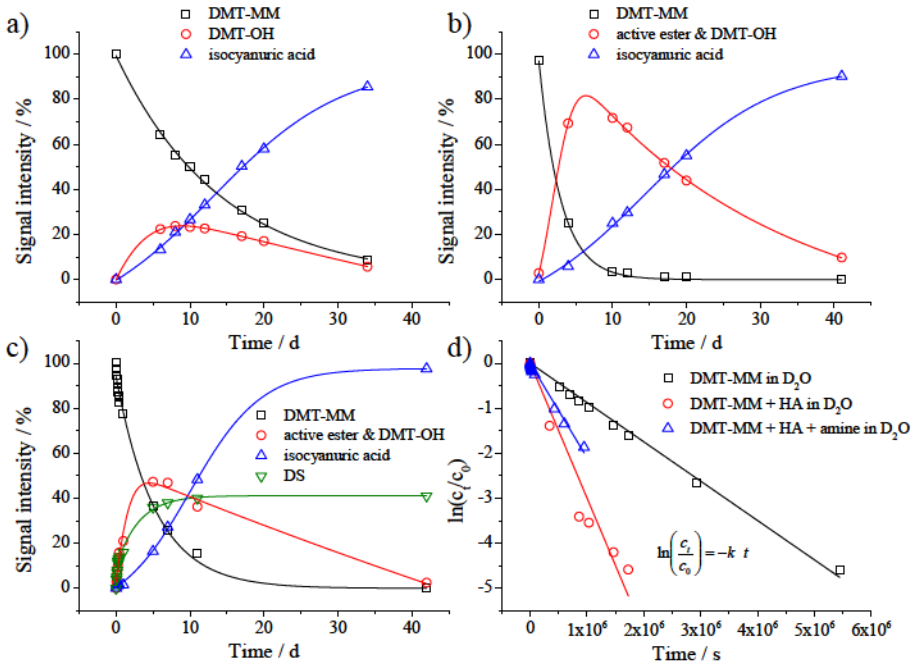

Figure 8 *^{1}H NMR kinetics of DMT-MM consumption and appearance of DMT-OH or active HA-ester as well as formation of isocyanuric acid derivative over time. The lines in graphs a)-c) are to guide the eye. a) DMT-MM hydrolysis in D_2O, b) DMT-MM +HA in D_2O, c) DMT-MM + HA + amine in D_2O. DS is the degree of substitution of amidated HA. d) First-order kinetic plot of DMT-MM consumption in presence and absence of HA and amine.*[1]

In the presence of propargyl amine, the "superactive ester" was immediately converted to the amide (Figure 8c). The rate of coupling agent consumption was similar in the amine mixture and in presence of HA alone (Figure 8d). Therefore, the amine had no accelerating effect on the formation of the HA-triazine ester. After about 10 h, the amidation rate slowed down, which was attributed to a change in acid-base equilibrium. The amine stoichiometry appeared to be the limiting factor for the DS, *i.e.* the use of 1.1 or 1.5 eq. of propargyl amine compared to HA carboxylate resulted in DS of 40 and 53 %, respectively. At higher initial reagent concentration relatively more deprotonated amines existed in the mixture, which was in accordance with previous findings.

HA-propargyl amide was obtained with the highest coupling efficiency at near stoichiometric reagent ratios and displayed excellent water solubility. The alkynyl moieties were stable upon storage and able to react orthogonally with azides in CuAAC. Hence the focus of further studies was placed on HA-propargyl derivatives for efficient grafting of side chains. The triazine-mediated amidation preserved on average 80 % of the molecular weight of the polysaccharide (Table 5).

Table 5 *Molecular weights and PDI of HA-amide derivatives.[a] (unpublished)*

Derivative	M_n / kg mol^{-1}	PDI	M_n / %
HA	422	1.15	100
HA-propargyl	331	1.26	78
HA-allyl	415	1.17	98
HA-thiol	284	1.36	67

[a]SEC in 0.1 M $NaNO_3$ calibrated with pullulan standards.

4.1.2 Esterification[III]

Esterification of HA was accomplished in a mixed solvent system (water/DMSO 1:3 v/v) without prior acidification of HA or counter ion exchange. The reaction was base catalyzed, using propargyl derivatives with a good leaving group, and stoichiometric reagent ratios. Propargyl bromide gave slightly higher DS compared with propargyl mesylate (Experimental, Table 2, entries 1&2), while no esterification was observed in mixtures with higher water content (Table 2, entry 4). The type of base had a strong effect on reaction outcome. Triethylamine (TEA) was more efficient in mediating the esterification than 1,8-diazabicyclo[5.4.0]undec-7-ene (DBU), supposedly due to its non-nucleophilic nature (Table 2, entries 1&5). DS were comparably high, varying between 17 and 40 %, and reactions at 45 °C for 24 h with 1 equivalent of TEA in respect to HA-carboxylate groups resulted in the least polysaccharide degradation with preservation of ~50 % of the molecular weight. Overall, the degradation was more pronounced during the esterification than amidation (Figure 9).

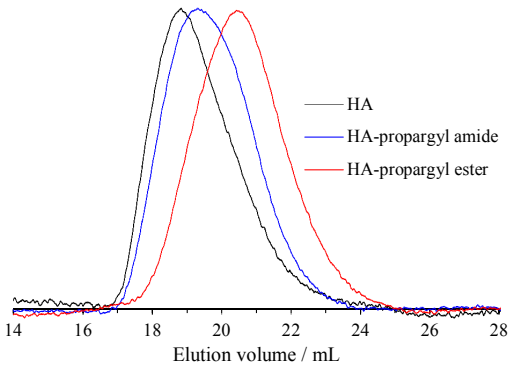

Figure 9 *SEC traces of HA and HA-propargyl amide and ester.[III]*

The ^{1}H NMR spectra of HA and HA-propargyl amide and ester are shown in Figure 10. As expected the propargyl ester signals were shifted downfield compared to the propargyl amide peaks due to deshielding induced by the electronegative oxygen.

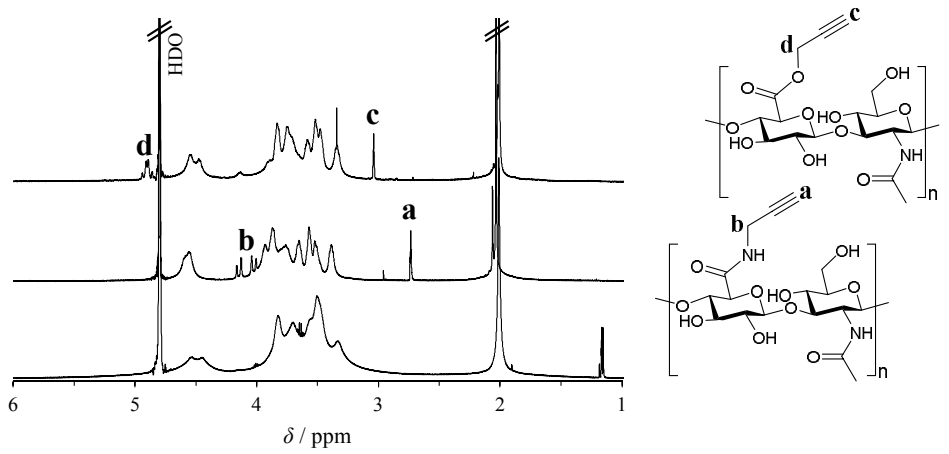

Figure 10 *^{1}H NMR spectra of (from bottom) HA, HA-propargyl amide and HA-propargyl ester in D_2O with chemical structures and assignment of characteristic peaks.*[I, III]

4.2 Synthesis of poly(glyceryl glycerol)

4.2.1 Ring-opening polymerization of IGG[II]

α-Azido-poly(glyceryl glycerol) (N_3-PGG) was synthesized by monomer-activated ring-opening polymerization (ROP) of (DL-1,2-isopropylidene glyceryl) glycidyl ether (IGG) in presence of triisobutylaluminum (Al-*i*Bu_3, Scheme 11). The polymerization mechanism relies on formation of a stoichiometric complex between the tetraalkylammonium initiator and Al-*i*Bu_3 and simultaneous activation of the epoxide monomer by coordination to Al-*i*Bu_3. Therefore the aluminum species has to be employed in excess compared to the initiator with the ratio depending on the structure of the monomer. Monomers consisting of multiple oxygen atoms, such as IGG, generate growing polymer chains with a tendency to complex aluminum, which is hence not available for activation.[132] For ROP of IGG (at a certain monomer concentration and targeting a certain DP) the optimal ratio of [Al-*i*Bu_3]:[initiator] was 4 (Experimental, Table 3). At lower ratios the reaction did not proceed to completion, while at higher ratios broadened molecular weight distributions were observed, due to aluminum-induced transfer reactions.

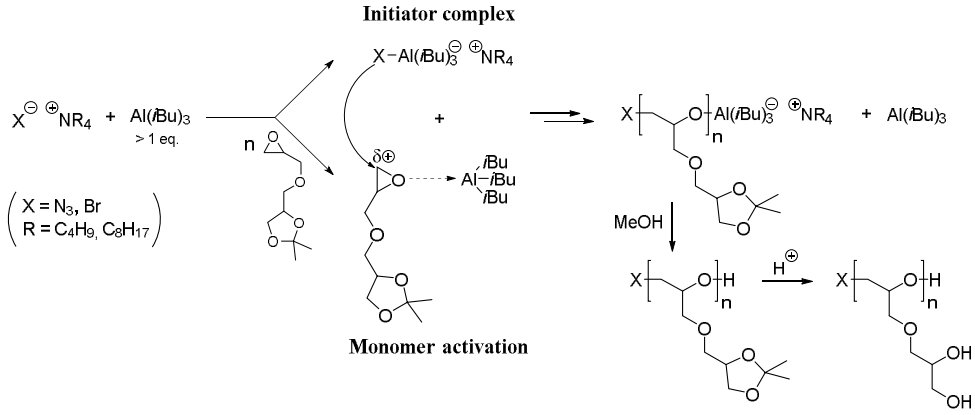

Scheme 11 *Mechanism of monomer-activated ROP of IGG and subsequent quenching and deprotection.*

Using this technique, polymers with higher degrees of polymerization (DP > 40) could be obtained than with previously reported methods (*i.e.* alkoxide initiated ROP).[129] Two different initiators were employed to obtain α-functional polymers. Tetrabutylammonium azide (NBu_4N_3) gave α-azido-PIGG directly, while use of tetraoctylammonium bromide ($NOct_4Br$) resulted in α-bromo-functional polymers. $NOct_4Br$ led to narrower molecular weight distribution of the products in accordance with the reported polymerization kinetics enhancing effect of larger counter ions (Figure 11). The bromide head group was easily substituted with sodium azide to yield the desired clickable polymers for grafting to HA-propargyl derivatives (Figure 12). The isopropylidene protecting groups were removed by acidic treatment to liberate the pendant 1,2-diol moieties.

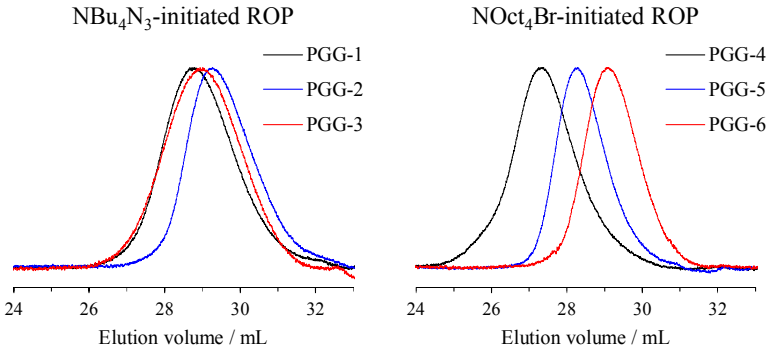

Figure 11 *SEC traces of PGGs polymerized with NBu_4N_3 (left) or $NOct_4Br$ (right).*[II]

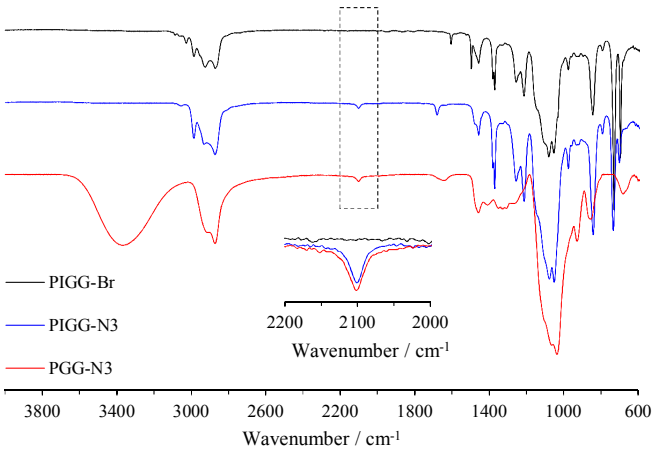

Figure 12 *FT-IR spectra of (from top) Br-PIGG, N_3-PIGG after substitution of the head group and N_3-PGG after deprotection. The azide peak is enlarged in the inset.*[II]

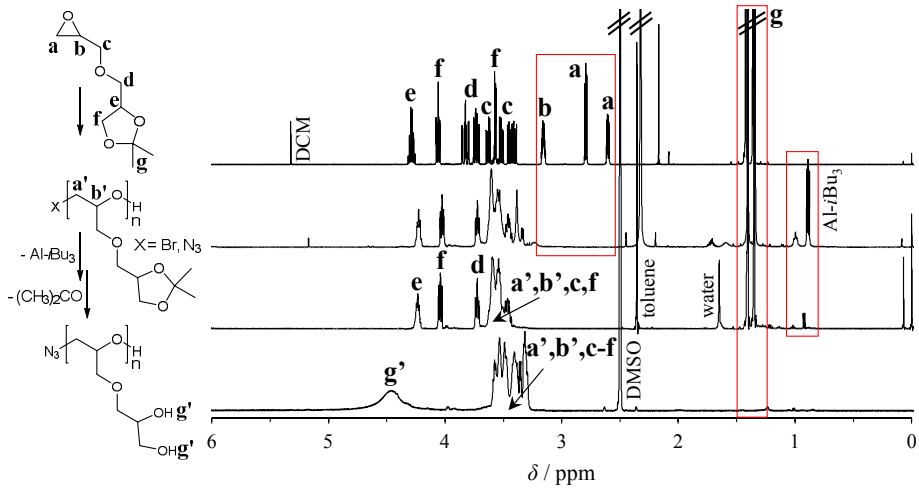

Figure 13 *^1H NMR spectra of (from top) IGG monomer, crude PIGG after polymerization, PIGG after precipitation of Al-iBu_3 and deprotected PGG. Frames highlight the signals that disappear after each step.*[II]

Figure 13 shows the ^1H NMR spectra of the monomer (IGG) and the crude polymer at 100 % conversion. Removal of the aluminum species by precipitation in diethyl ether as well as successful deprotection were confirmed by NMR. The molecular weights of the protected polymers (PIGGs) were close to the theoretical values, according to SEC against polystyrene standards and assuming that every initiator molecule starts one polymer chain

(Experimental, Table 3). The molecular weights of deprotected PGGs are underestimated, due to the difference in solution properties of linear poly(ethylene oxide) standards and the compact, side chain substituted polyglycerols.[112] The prepared PGG chains (~10 kg mol^{-1}) have molecular weights well below the renal threshold reported for PEG (~30 kg mol^{-1})[133] and possess around 130 hydroxyl groups for conjugation with drugs, probes and targeting ligands.

4.2.2 Functionalization of PGG

In contrast to PEG, PGG is only soluble in polar solvents, such as water, DMSO, DMF, *N*-methyl-2-pyrrolidone, methanol, ethanol, and pyridine. Therefore the conjugation of PGG with drugs, probes and targeting molecules is more challenging. Different strategies were explored to functionalize PGG with model compounds.

4.2.2.1 Pyrene-ether of PGG[III]

1-Bromomethylpyrene was conjugated to PGG by Williamson ether synthesis to act as both a fluorescent tag for release studies and as a hydrophobic model compound. PGG-pyrene was found to contain 0.12 mol% of the tag per PGG repeating unit or 7.9 µg pyrene per 1 g polymer as determined by UV and ^{1}H NMR. The modification had no effect on the molecular weight distribution of the polymer (Figure 14a). PGG-conjugated pyrene showed increased water solubility compared with uncoupled pyrene, but maintained its characteristic UV and fluorescence properties (Figure 14b). No excimer fluorescence was observed in the studied concentration range (up to 10 mg mL^{-1} polymer concentration), indicating that the pyrene moieties were randomly distributed along the polymer chain.

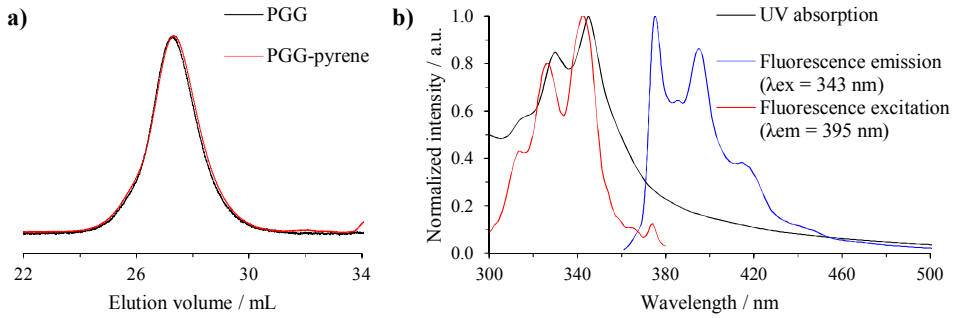

Figure 14 *a) SEC traces of PGG-pyrene and its precursor polymer. b) UV and fluorescence spectra of PGG-pyrene in PBS.[III]*

4.2.2.2 Boronic ester of PGG[II]

Compared with polyglycerol, PGG has the ability to form dynamic covalent bonds with boronic acid derivatives. The pendent 1,2-diol groups in PGG spontaneously reacted with boronic acids to boronic esters under liberation of water (Scheme 12). NMR spectra of an equimolar mixture of PGG diols and phenylboronic acid (PBA) in deuterated methanol (MeOD) showed the appearance of new signals attributed to boronate-bound PGG repeating units (4.0 - 4.7 ppm), as well as shifts in the aromatic peaks of PBA (Figure 15a). The new signals had similar translational diffusion coefficients as the PGG backbone in diffusion-ordered (DOSY) NMR spectra, thus proving their attachment to the polymer (Figure 15b). Integration of the signals gave the equilibrium degree of esterification of 33 % under the given conditions.

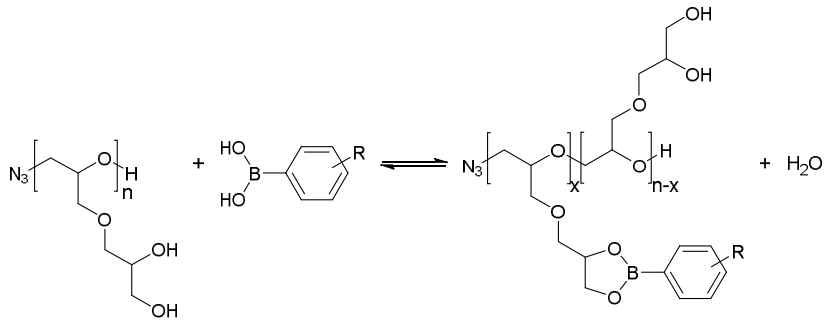

Scheme 12 *Boronic ester formation between PGG and a boronic acid derivative.*

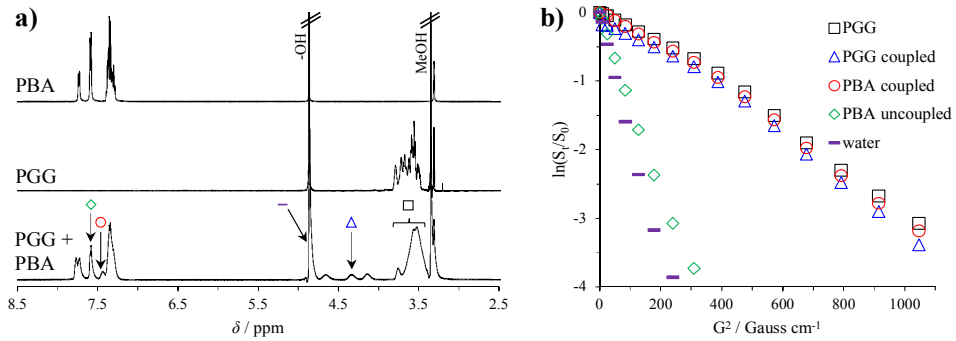

Figure 15 *a) [1]H NMR spectra of (from top) PBA, PGG and an equimolar mixture of PGG/PBA in MeOD. b) Signal intensity versus gradient strength of peaks in the PGG/PBA mixture marked in a) determined by DOSY NMR (diffusion delay 100 ms, 16 spectra with linearly incremented gradient strength). Diffusion coefficients were calculated from the slope of the curves.[II]*

PGG boronic ester formation was further demonstrated under physiologically relevant conditions (PBS, pH 7.4). Although literature reports have described glycerol boronic esters as weak and hydrolytically unstable,[134] the interaction of PGG with rhodamine B boronic acid was found to be strong enough for efficient fluorescence labeling of the polymer (Table 6). PGG chains were anchored at the surface of model polymeric nanoparticles to facilitate their separation from uncoupled dye molecules. Therefore, PGG was conjugated to hydrophobic poly(L-lactide) (PLLA) via CuAAC. The amphiphilic block copolymers were assembled into particles of 70 nm diameter by nanoprecipitation into PBS. The formed particles displayed a PGG corona that could be functionalized post-assembly by simple addition of boronic acids. PGG particles were mixed with 10 mol% of a dye compared to diol concentration and then extensively dialyzed. With rhodamine B boronic acid, 86 % of the dye was retained after dialysis, while plain rhodamine B was completely removed. The high labeling efficiency (LE) was ascribed to the favorable interactions in polyols, *i.e.* steric bulk hindering the attack of water and thus hydrolysis, as well as favorable entropy due to the large number of possible boronic esters and isomers.[135]

Table 6 *Labeling efficiency (LE) of PGG particles with rhodamine B boronic acid or rhodamine B after extensive dialysis.*[II]

Sample	c_0[a] / 10^{-5} M	c_{dye}[b] / 10^{-5} M	LE / %
Rhodamine B boronic acid	28.7	24.6	85.5
Rhodamine B	28.7	0.06	0.2

[a]Theoretical dye concentration in a 1 mg mL^{-1} dispersion of PGG particles. [b]Experimental dye content in a 1 mg mL^{-1} dispersion of PGG particles after extensive dialysis determined by fluorescence spectroscopy.

Boronic ester formation between PGG and functional boronic acids is an attractive strategy for fast and simultaneous conjugation of multiple probes and targeting moieties under mild conditions. The strategy is also applicable to specific labeling of PGG in HA-PGG graft copolymers, as HA does not feature the reactive *cis*-diol motif. The stability of PGG boronic esters in presence of diol-containing biomolecules, such as carbohydrates or glycoproteins, needs further investigation to evaluate the usefulness of the approach for targeted drug delivery.

4.2.2.3 PGG-hydrazide

Hydroxyl groups exhibit a relatively low nucleophilicity compared to other functional groups (*e.g.* amines, carboxylates, and thiols) and their modification is often complicated in the presence of water. To achieve efficient coupling of PGG with bioactive molecules, its pendant hydroxyl groups were converted into more reactive moieties. PGG was first reacted with methyl bromoacetate in another Williamson ether synthesis and subsequently aminolyzed with hydrazine to yield hydrazide groups. Hydrazides can be conjugated with

aldehyde/ketone groups in drug molecules (*e.g.* dexamethasone) leading to acid-labile hydrazones, or they can react with activated carboxyls or isothiocyanates to form amide or thiourea derivatives (Scheme 13). Hence, PGG-hydrazide enables the coupling of many commercially available probes and targeting ligands.

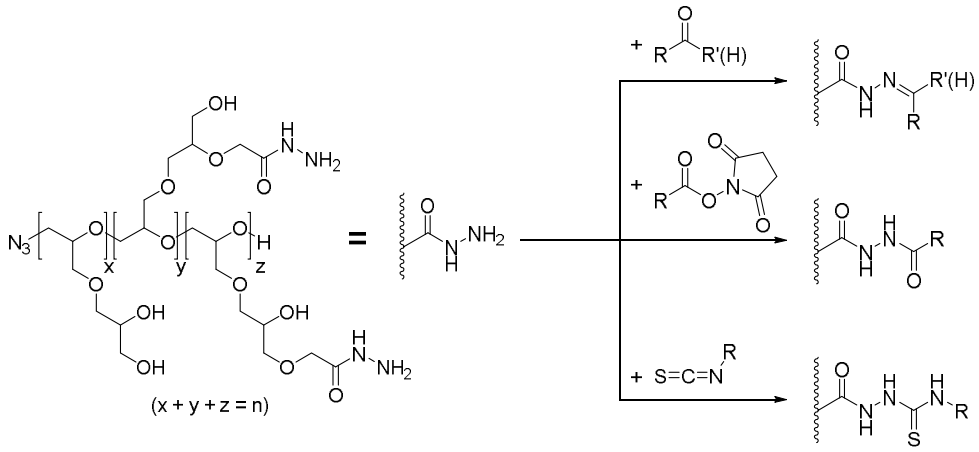

Scheme 13 *Possible pathways for functionalization of PGG-hydrazide with drugs, probes and targeting moieties: (from top) hydrazone formation with aldehydes/ketones, amidation with active ester derivatives, thiourea formation with isothiocyanates.*

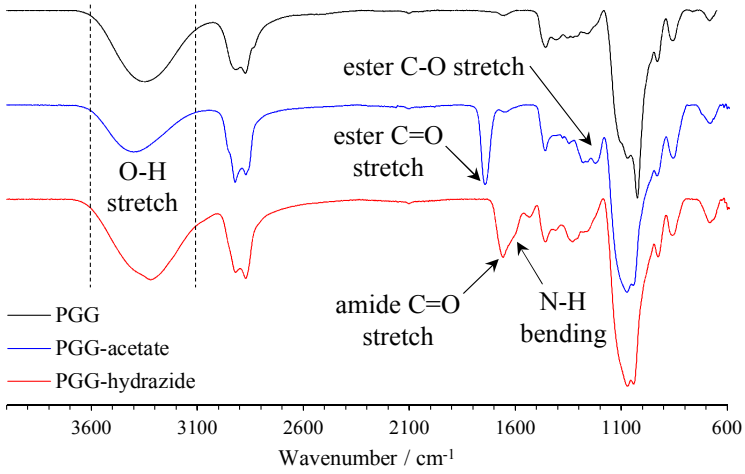

Figure 16 *FT-IR spectra of (from top) PGG, PGG-acetate and PGG-hydrazide with assignment of characteristic signals. (unpublished)*

DS obtained ranged between 20 and 42 % of hydrazide per PGG repeating unit, which corresponds to about 15-28 hydrazide groups per polymer chain (DP = 67). Full conversion of the hydroxyl groups was impeded by the partial insolubility of PGG-alkoxides in DMF during the ether synthesis. The acetylated PGG derivative was insoluble in common solvents and could only be analyzed by FT-IR spectroscopy. However, Figure 16 shows a reduction in hydroxyl peak intensity in PGG-acetate compared to PGG, as well as a strong ester carbonyl stretching band at 1744 cm^{-1} and C-O stretching bands at 1223 and 1280 cm^{-1}. After hydrazinolysis, the carbonyl stretching peak in PGG-hydrazide was shifted completely to the amide frequency (1658 cm^{-1}), and N-H bending (1600 cm^{-1}) and stretching (3319 cm^{-1}) bands appeared. PGG-hydrazide was soluble in DMSO and water.

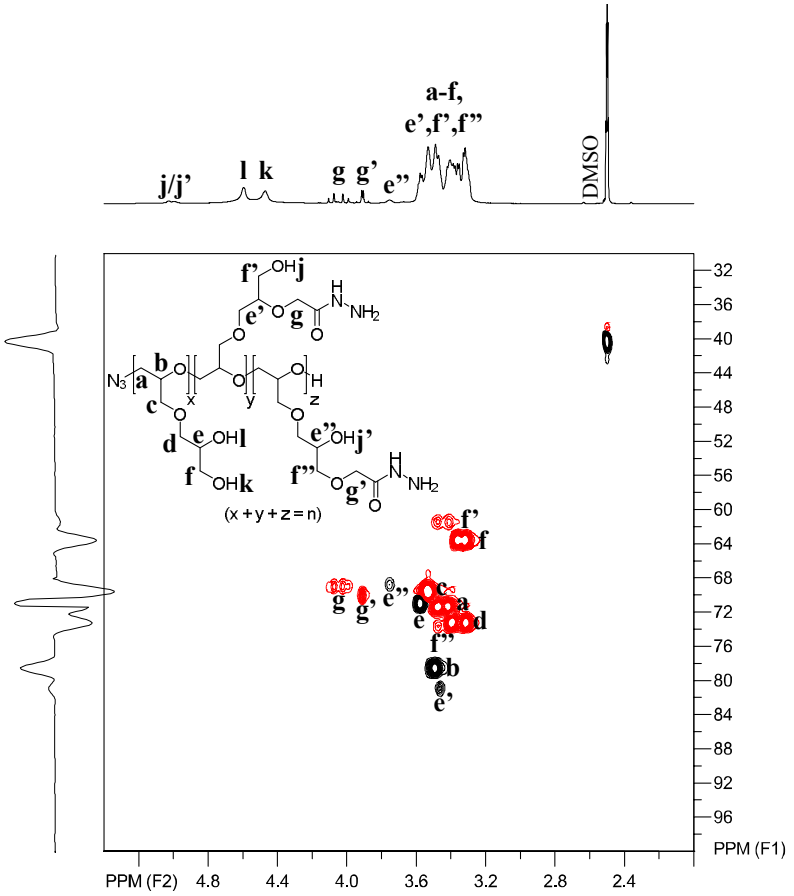

Figure 17 *HSQC NMR of PGG-hydrazide in DMSO-d_6. Inset shows the structure and peak assignment. (unpublished)*

The structure of PGG-hydrazide was confirmed by NMR spectroscopy. Figure 17 shows the heteronuclear single quantum coherence (HSQC) NMR spectrum of PGG-

hydrazide in DMSO-d_6. The peaks were assigned based on homo- and heteronuclear correlation spectra (data not shown).

4.3 Grafting of PGG onto HA[III]

4.3.1 Click reaction conditions

Prior to grafting of N_3-PGG onto HA-propargyl derivatives, different CuAAC reaction conditions were tested for their potential to degrade HA. It is known that *in situ* reduction of copper(II) sulfate by sodium ascorbate to produce the catalytically active Cu^+ species creates hydroxyl radicals, which degrade HA.[136] The same was observed in this study. Figure 18 shows the SEC traces of HA-propargyl ester derivatives treated under click reaction conditions with sodium azide as a model reaction partner to avoid changing the solution properties of the polysaccharide. The derivative treated with Cu(II) and ascorbate retained only about 25 % of its original molecular weight, while a reaction using copper(I) bromide and a ligand in water/DMSO (1:3 v/v) preserved 71 % of the molecular weight. Therefore the grafting was conducted using the latter conditions.

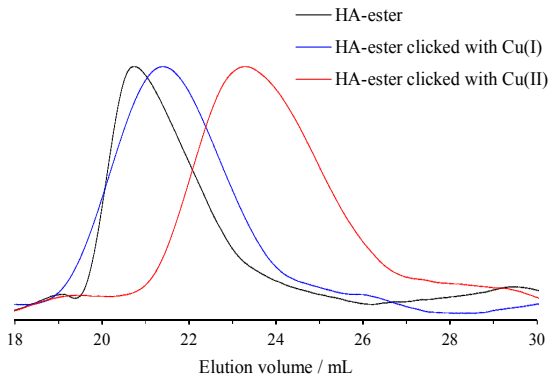

Figure 18 *SEC traces of HA-propargyl ester and HA derivatives after model click reactions catalyzed by copper(I) bromide or copper(II) sulfate / ascorbic acid.*[III]

PGG-pyrene was grafted to HA-propargyl ester to obtain a fluorescently labeled graft copolymer with hydrolysable bonds for release studies (Scheme 14). Upon grafting, the ^{1}H NMR peaks of the HA-propargyl moieties disappeared and the characteristic signals of the triazole ring and the adjacent methylene group appeared (Figure 19), proving the success of the reaction.

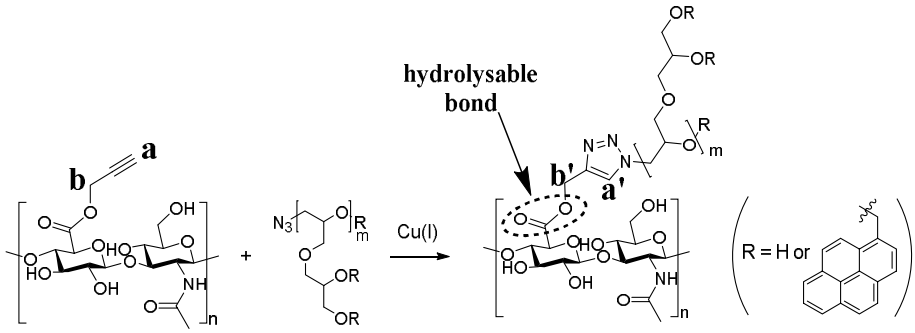

Scheme 14 *Click grafting of PGG-pyrene onto HA-propargyl ester.*

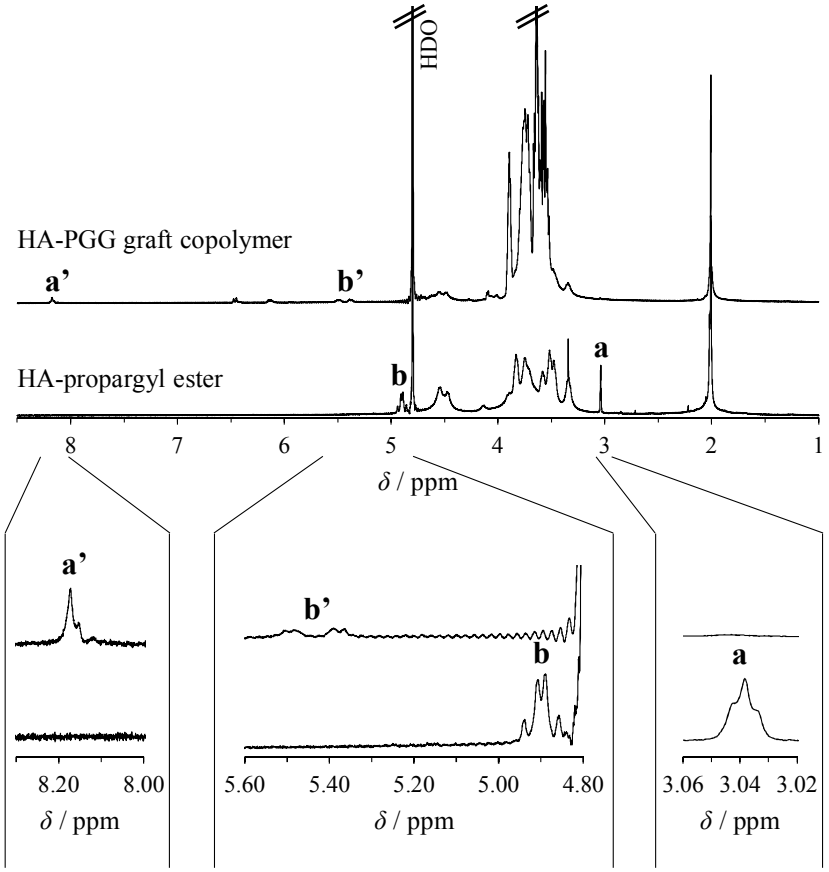

Figure 19 *[1]H NMR spectra of HA-propargyl ester and HA-PGG graft copolymer after click reaction. The spectral areas where peak shifts occur are enlarged. Peaks are assigned according to Scheme 14.[III]*

4.3.2 Purification of HA-PGG graft copolymers

SEC measurements of HA-PGG showed an increase in molecular weight of the graft copolymer compared to HA-propargyl ester (Figure 20). The shift to lower elution volumes was rather small and attributed to the flexible and compact nature of PGG. The measurements also revealed an excess of uncoupled PGG chains that were not removed by dialysis (using a 25 kg mol^{-1} MWCO to remove 3.1 kg mol^{-1} uncoupled PGG). The majority of uncoupled PGG could be removed by extraction of the lyophilized copolymer with methanol, which is a non-solvent for HA but dissolves PGG. In order to ensure accurate release results, the content of uncoupled PGG in the studied material was always determined at the start of the experiment (t = 0).

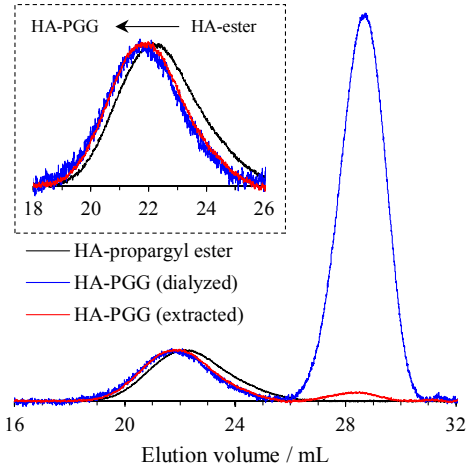

Figure 20 *SEC traces of HA-propargyl ester and HA-PGG click product after purification by dialysis and extraction.*[III]

4.4 Release studies[III]

The properties of HA-propargyl derivatives and HA-PGG ester graft copolymers were studied under simulated physiological conditions. The materials were incubated in either PBS or 10 % (v/v) porcine vitreous liquid in PBS at pH 7.4 and 37 °C. Changes in the molecular weight and chemical structure of the materials were investigated and their biocompatibility was tested in cell cultures.

4.4.1 Stability of HA derivatives during incubation

HA and HA-propargyl derivatives were incubated for 36 days to estimate the extent of polysaccharide backbone degradation via non-enzymatic and enzymatic hydrolysis. Neither native HA nor HA derivatives showed pronounced degradation during the experiment. The SEC traces of HA-propargyl ester were slightly shifted to higher elution volumes (Figure 21a), supposedly due to the loss of the propargyl linker upon ester hydrolysis. The magnitude of the shift was the same in PBS and vitreous-containing buffer. The molecular weight distribution of HA-propargyl amide remained unchanged after incubation in PBS, but the peak maximum was shifted slightly after incubation in vitreous (Figure 21b). A similar behavior was observed for native HA. The overall degradation of the polysaccharides was found to be negligible and will not affect the release of side chains from the graft copolymer.

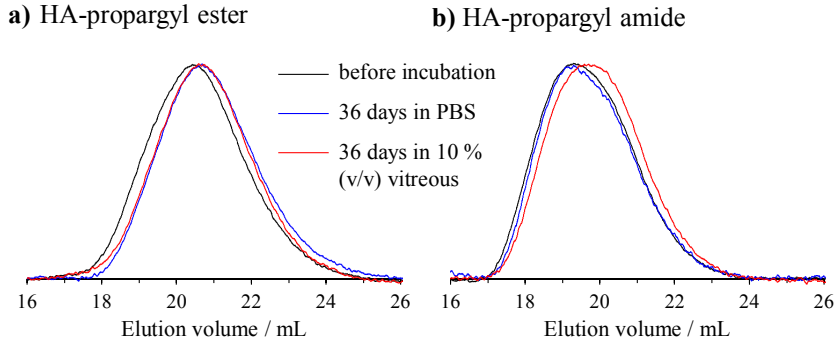

Figure 21 *SEC traces of HA-propargyl ester (a) and amide (b) before and after incubation in PBS or 10 % (v/v) vitreous liquid in PBS at 37 °C for 36 days.*[III]

The structural changes of the HA-derivatives upon incubation were studied by NMR spectroscopy. The propargyl ester was completely cleaved after 36 days of incubation in both media, while the propargyl amide was still intact (Figure 22). The area of the propargyl amide signal decreased from about 40 % DS to roughly 30 % DS, indicating slow hydrolysis of the linkage.

4.4.2 Release kinetics

The kinetics of HA-propargyl ester hydrolysis were studied *in situ* by NMR spectroscopy. The derivative was incubated in PBS containing 5 % (v/v) D_2O at 37 °C to emulate the conditions used in the release experiments. Hence, ^1H NMR spectra had to be acquired using a water suppression pulse sequence. The signals of propargyl ester (~3.0 ppm) and its hydrolysis product, propargyl alcohol (~2.8 ppm), were followed with time. Half-life of the HA-propargyl ester was found to be about 3.9 h (Table 8). The value was in

accordance with the report of a more hydrophobic HA-corticosteroid ester, which exhibited $t_{1/2} \sim 6.5$ h.[137]

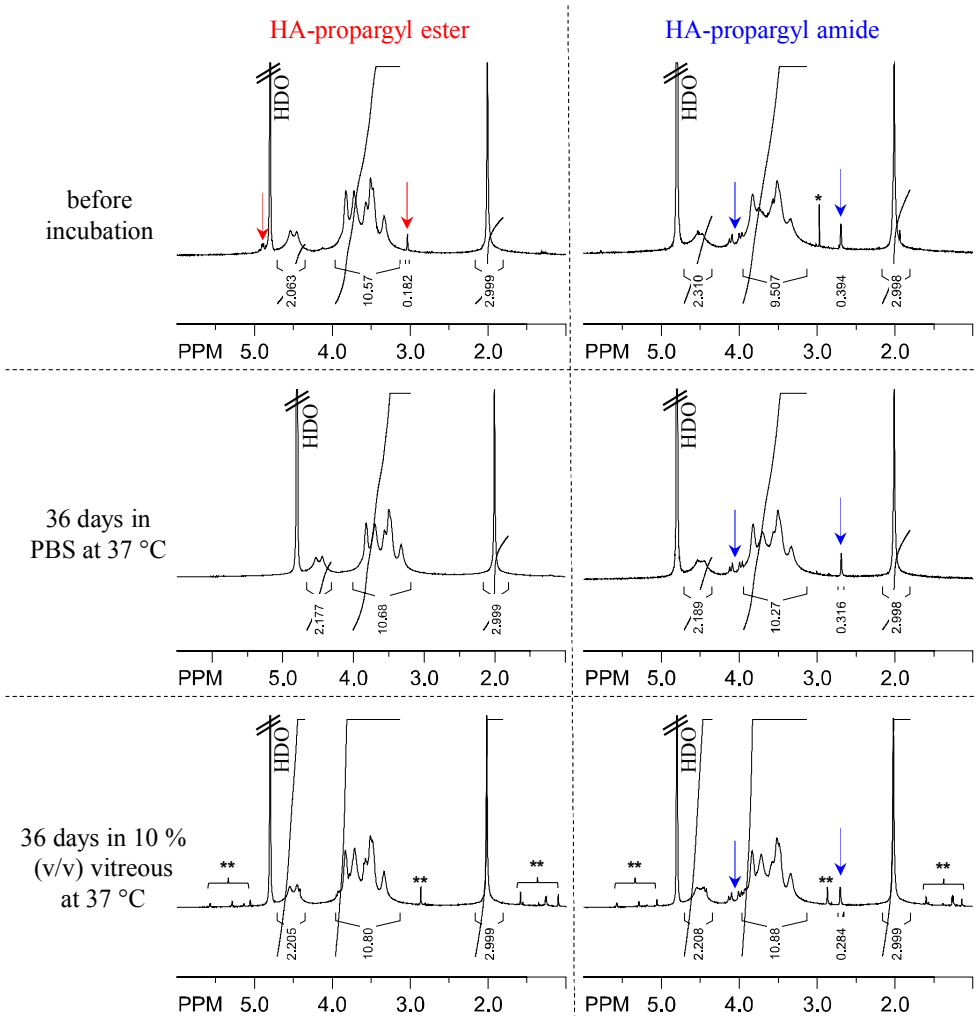

Figure 22 *^{1}H NMR spectra of HA-propargyl ester (left) and amide (right) before (top) and after incubation in PBS (middle) or 10 % (v/v) vitreous liquid in PBS (bottom). Propargyl peaks are marked with arrows. *N-methylmorpholinium impurity from amidation. **Signals originating from the vitreous.*[III]

The polymer-from-polymer release of PGG grafts from the ester-linked HA-PGG graft copolymer was investigated using two types of setups. Pyrene-modified PGG was used to enable detection of released chains. All experiments were conducted in PBS at 37 °C. First, in a dialysis setup released PGG-pyrene was separated from the incubation mixture by diffusion across the membrane. The concentration of PGG-pyrene in the dialysate was

determined by fluorescence. Second, the composition of the incubation mixture was measured directly by SEC. Samples were withdrawn at specific time points and subjected to SEC measurements. The amount of released PGG-pyrene was determined by integration of the PGG elution peak.

The permeability of PGG-pyrene (9.2 kg mol^{-1}) across the membranes of two different dialysis devices (MWCO ~20 kg mol^{-1}; Experimental, Figure 6) was studied. The combination of miniaturized dialysis setups and fluorescence detection can significantly reduce the amount of polymer material required for release experiments. Furthermore, the high ratio of membrane surface area to sample volume (SA:V) in these devices can increase the rate of analyte permeation. PGG-pyrene was completely released from the Slide-A-Lyzer® device after 48 h, while the majority of the polymer was still trapped within the QuixSep® device (Figure 23a). The difference in dialysis efficiency was likely due to the 5-times larger SA:V ratio of the Slide-A-Lyzer® in this specific experiment (Table 7).

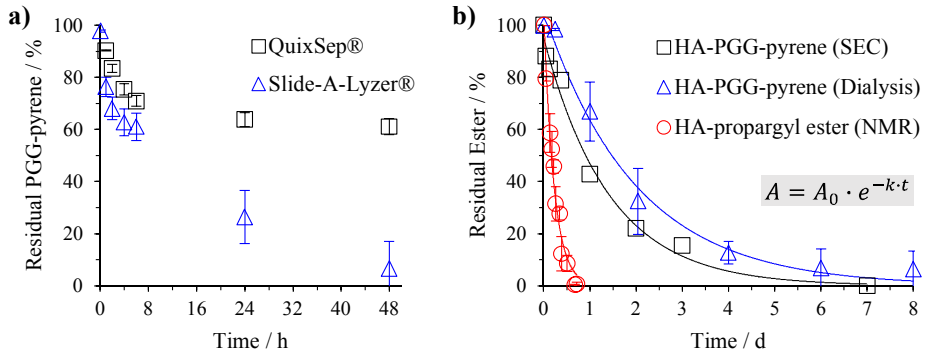

Figure 23 *Release kinetics determined in PBS at 37 °C: a) Release of PGG-pyrene from QuixSep® or Slide-A-Lyzer®. b) Release of PGG-pyrene from the HA graft copolymer studied by SEC and dialysis (Slide-A-Lyzer®), and cleavage of ester bonds in HA-propargyl ester studied by ^{1}H NMR. Data is reported as mean (n=2-3) ± standard deviation and fitted with the integrated ester hydrolysis rate law shown in b).*[III]

Table 7 *Characteristics of dialysis devices.*[III]

Dialysis device	MWCO / kg mol^{-1}	Sample / µL	Dialysate / mL	Volume ratio	Membrane surface area / cm^2	SA:V[a] / cm^2 mL^{-1}
QuixSep®	25	800.0	30	37.5	1.77	2.21
Slide-A-Lyzer®	20	26.7	1	37.5	0.28	10.59

[a]Surface area-to-volume ratio.

The release of PGG-pyrene from the HA graft copolymer was complete after 1 week in both release experiments (dialysis and SEC, Figure 23b). In case of the SEC study, the rate of ester bond hydrolysis was determined by fitting of the data with the integrated ester hydrolysis rate law (see inset of Figure 23b). The data obtained from the dialysis study was fitted with equation (4), taking into account the different setup. The appearance of free PGG-pyrene in the dialysate is governed by two processes, *i.e.* hydrolysis of the HA-PGG graft copolymer within the dialysis device (equation (1)) and diffusion of free PGG across the membrane (equation (3) and Figure 24). This can be considered as a consecutive reaction, and thus the individual rate constants of hydrolysis and diffusion ($k_{hydr.}$ and $k_{diff.}$) could be separated. The obtained $k_{hydr.}$ was in excellent agreement with the rate constant determined in the SEC experiment (Table 8).

(1) $$\frac{d[PGG]_{bound}}{dt} = -k_{hydr} \cdot [PGG]_{bound}$$

(2) $$\frac{d[PGG]_{free}}{dt} = k_{hydr} \cdot [PGG]_{bound} - k_{diff} \cdot [PGG]_{free}$$

(3) $$\frac{d[PGG]_{dialysate}}{dt} = k_{diff} \cdot [PGG]_{free}$$

(4) $$[PGG]_{dialysate} = \left\{1 + \frac{k_{hydr} \cdot e^{-k_{diff} \cdot t} - k_{diff} \cdot e^{-k_{hydr} \cdot t}}{k_{diff} - k_{hydr}}\right\} \cdot [PGG]_{bound}$$

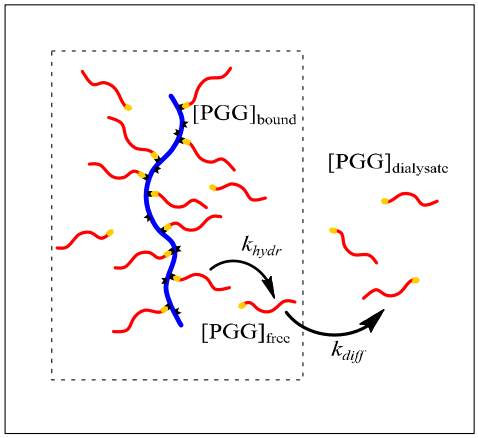

Figure 24 *Model describing the consecutive release of PGG from the graft copolymer and subsequent diffusion from the dialysis device.*[III]

Table 8 *Hydrolysis and diffusion rate constants, as well as half-lives of HA derivatives in PBS at 37 °C.*[III]

	k_{hydr} / 10^{-2} h^{-1}	k_{diff} / 10^{-2} h^{-1}	$t_{1/2}$[a] / h	adj. R^2 [b]
HA-PGG-pyrene (SEC)	2.95 ± 0.27	-	23.51 ± 2.19	0.986
HA-PGG-pyrene (Dialysis)	2.97 ± 0.38	10.50 ± 3.31	23.34 ± 3.04	0.997
HA-propargyl ester (NMR)	17.63 ± 1.00	-	3.93 ± 0.22	0.970

[a]The half-life was calculated according to $t_{1/2} = \ln(2) / k_{hydr.}$ [b]Coefficient of determination adjusted by the degrees of freedom of the fit model.

The hydrolysis of the HA-PGG graft copolymer ($t_{1/2}$ ~23.4 h) was considerably slower than that of the HA-propargyl ester derivative ($t_{1/2}$ ~3.9 h). The slow release of polymeric side chains, as compared to small molecular linkers, was attributed to steric crowding in the graft copolymer, shielding the ester bonds from attack by water molecules. A graft copolymer with cleavable drug-carrying polymer side chains thus has the potential to achieve longer lasting release than a mere prodrug with drug molecules attached to the backbone.

4.4.3 Biocompatibility

Biocompatibility studies were performed with the HA-PGG graft copolymer and PGG grafts. The viability of different cell lines after incubation with polymers was investigated by MTT cytotoxicity assay. Human retinal pigment epithelial cells (ARPE-19) and human umbilical vein endothelial cells (HUVEC) were selected for their relevance in ocular drug development. Monkey kidney fibroblasts (CV-1) and human ovarian adenocarcinoma cells (SKOV-3) were studied to assess the general cytotoxicity of the materials toward healthy and diseased cells. The cells were incubated with different concentrations of polymers for 5 h and in growth medium for 20 h. The metabolic activity of the cells was measured spectrophotometrically after addition of 3-(4,5-dimethylthiazol-2-yl)-2,5-diphenyl-tetrazolium bromide (MTT), which is reduced to purple formazan in the mitochondria of living cells.

The cell viability after incubation with HA-PGG or PGG was compared with the response induced by polyvinyl alcohol (PVA), which is non-toxic and FDA-approved for ocular use, and branched poly(ethylene imine) (PEI), which is known to be cytotoxic. HA-PGG and PGG exhibited similar levels of cell viability to PVA for concentrations up to 0.1 mg mL^{-1} (Figure 25), which is the envisioned concentration in the vitreous after injection. At higher concentrations both polymers decreased the cell viability compared to PVA, although HA-containing polymers were better tolerated. The effect may originate from residual impurities from the synthesis, especially the copper-mediated click grafting. Metal impurities may be further reduced by filtration over an ion exchange resin. The polymers were much less toxic than PEI and are thus considered promising biomaterials.

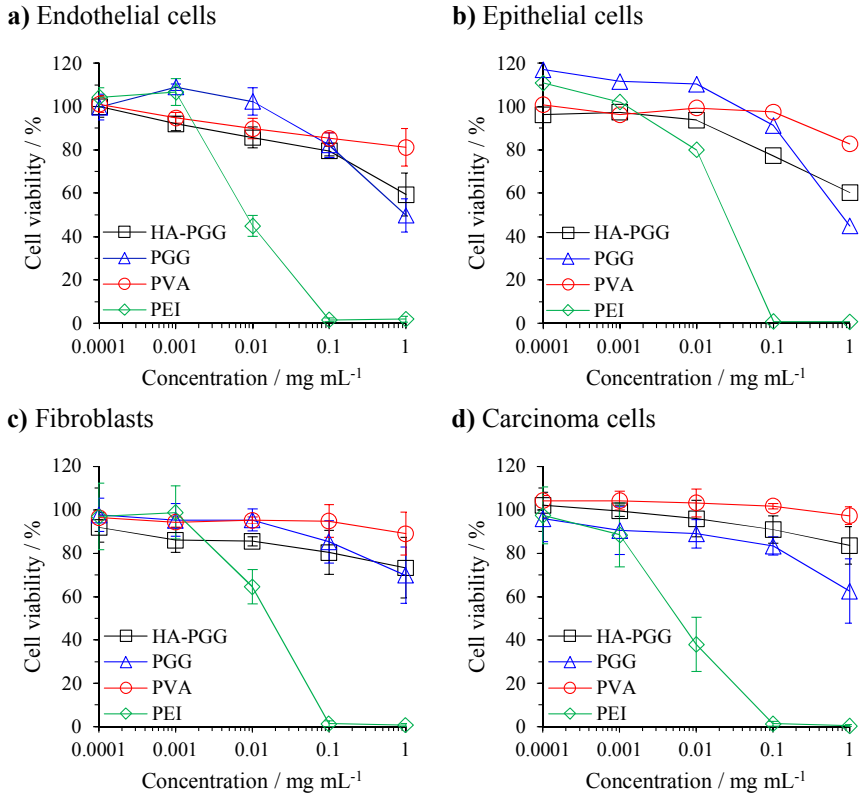

Figure 25 *Cell viability versus polymer concentration determined by MTT assay of a) human retinal pigment epithelium (ARPE-19), b) human umbilical vein endothelial cells (HUVEC), c) monkey kidney fibroblasts (CV-1), and d) human ovarian adenocarcinoma cells (SKOV-3). Cells were incubated with HA-PGG graft copolymer, PGG, FDA-approved PVA or cytotoxic PEI. Data is presented as mean of three experiments (except HUVEC) ± standard deviation.*[III]

5 Conclusions

The synthesis of water-soluble hyaluronic acid (HA) graft copolymers was studied in detail and the suitability of the copolymers as vehicles for intravitreal drug delivery was examined. High molecular weight HA was modified with clickable propargyl-linkers for *grafting onto* of multifunctional side chains. The linkers were introduced via amidation or esterification to yield stable or hydrolysable bonds. The reaction conditions were optimized to reduce HA degradation and to yield comparatively high degrees of substitution at stoichiometric reagent ratios. Amidation was found to induce less degradation of HA than esterification.

Complementary click functional side chains were prepared by monomer-activated ring-opening polymerization of protected glycidyl ethers. The resulting polymers were α-azido-polyethers with pendant 1,2-diol moieties in every repeating unit, *i.e.* poly(glyceryl glycerol) (PGG). Using a Lewis acid catalyst, degrees of polymerization of PGG >40 were achieved for the first time, resulting in polymers with >100 pendant functional groups and molecular weights below the renal threshold. The diols were amenable to labeling with boronic acid derivatives with high efficiency in neutral aqueous solution. Part of the PGG hydroxyls were further converted into reactive hydrazide groups for subsequent attachment of drugs and into pyrene ethers for detection in release studies. Grafting of PGG onto HA-propargyl ester was achieved by copper-mediated azide-alkyne cyclo-addition, producing water-soluble graft copolymers with cleavable arms.

The materials were incubated under simulated vitreal conditions to determine their stability and release behavior. HA and its derivatives showed no sign of polysaccharide degradation within a month. HA-propargyl esters were completely cleaved after 1 week, while amide bonds remained mostly intact. Hydrolysis of propargyl esters was followed by NMR, whereas polymer-from-polymer release of PGG grafts from the HA-PGG ester graft copolymer was studied by SEC and dialysis. The rate of cleavage of PGG chains was significantly lower than the hydrolysis of the small molecular propargyl linker, and was attributed to steric crowding at the ester carbonyl. Biocompatibility tests were performed in cell cultures. PGG and HA-PGG graft copolymers exhibited similar levels of cell viability as polyvinyl alcohol, a FDA-approved polymer for ocular use.

Thus, HA-based graft copolymers with cleavable arms are promising materials for intravitreal drug delivery applications. They have the potential to achieve long retention times in the vitreous due to their high molecular weight. The slow cleavage of polymer grafts allows for longer-lasting release than a direct release of drugs from a polymer. Using the presented strategies, the grafts can be further conjugated with drugs, probes and targeting ligands, and tested in ophthalmic applications.

6 References

(1) Duncan, R.; Kopeček, J. Soluble Synthetic Polymers as Potential Drug Carriers. In *Polymers in Medicine*; Advances in Polymer Science; Springer, Berlin, Heidelberg, 1984; pp 51–101.
(2) Hoste, K.; De Winne, K.; Schacht, E. Polymeric Prodrugs. *Int. J. Pharm.* **2004**, *277* (1), 119–131.
(3) Liu, S.; Maheshwari, R.; Kiick, K. L. Polymer-Based Therapeutics. *Macromolecules* **2009**, *42* (1), 3–13.
(4) Ringsdorf, H. Structure and Properties of Pharmacologically Active Polymers. *J. Polym. Sci. Polym. Symp.* **1975**, *51* (1), 135–153.
(5) Takakura, Y.; Mahato, R. I.; Nishikawa, M.; Hashida, M. Control of Pharmacokinetic Profiles of Drug—macromolecule Conjugates. *Adv. Drug Deliv. Rev.* **1996**, *19* (3), 377–399.
(6) Larson, N.; Ghandehari, H. Polymeric Conjugates for Drug Delivery. *Chem. Mater.* **2012**, *24* (5), 840–853.
(7) Ouchi, T.; Ohya, Y. Macromolecular Prodrugs. *Prog. Polym. Sci.* **1995**, *20* (2), 211–257.
(8) Khandare, J.; Minko, T. Polymer–drug Conjugates: Progress in Polymeric Prodrugs. *Prog. Polym. Sci.* **2006**, *31* (4), 359–397.
(9) Seymour, L. W.; Duncan, R.; Strohalm, J.; Kopeček, J. Effect of Molecular Weight (Mw) of N-(2-Hydroxypropyl)Methacrylamide Copolymers on Body Distribution and Rate of Excretion after Subcutaneous, Intraperitoneal, and Intravenous Administration to Rats. *J. Biomed. Mater. Res.* **1987**, *21* (11), 1341–1358.
(10) Garg, H. G.; Hales, C. A. *Chemistry and Biology of Hyaluronan*; Elsevier: Amsterdam; Boston, 2004.
(11) Hu, Y.; Li, Y.; Xu, F.-J. Versatile Functionalization of Polysaccharides via Polymer Grafts: From Design to Biomedical Applications. *Acc. Chem. Res.* **2017**, *50* (2), 281–292.
(12) Jeong, Y.-I.; Choi, K.-C.; Song, C.-E. Doxorubicin Release from Core-Shell Type Nanoparticles of Poly(DL-Lactide-Co-Glycolide)-Grafted Dextran. *Arch. Pharm. Res.* **2006**, *29* (8), 712.
(13) Lee, H.; Ahn, C.-H.; Park, T. G. Poly[Lactic-Co-(Glycolic Acid)]-Grafted Hyaluronic Acid Copolymer Micelle Nanoparticles for Target-Specific Delivery of Doxorubicin. *Macromol. Biosci.* **2009**, *9* (4), 336–342.
(14) Meng, X.; Edgar, K. J. "Click" Reactions in Polysaccharide Modification. *Prog. Polym. Sci.* **2016**, *53* (Supplement C), 52–85.
(15) Sen, G.; Sharon, A.; Pal, S. Grafted Polysaccharides: Smart Materials of the Future, Their Synthesis and Applications. In *Biopolymers*; Kalia, S., Avérous, L., Eds.; John Wiley & Sons, Inc., 2011; pp 99–127.
(16) Gu, C.; Le, V.; Lang, M.; Liu, J. Preparation of Polysaccharide Derivates Chitosan-Graft-Poly(ε-Caprolactone) Amphiphilic Copolymer Micelles for 5-Fluorouracil Drug Delivery. *Colloids Surf. B Biointerfaces* **2014**, *116* (Supplement C), 745–750.
(17) Atanase, L. I.; Desbrieres, J.; Riess, G. Micellization of Synthetic and Polysaccharides-Based Graft Copolymers in Aqueous Media. *Prog. Polym. Sci.* **2017**, *73* (Supplement C), 32–60.
(18) Wang, Z.-H.; Zhu, Y.; Chai, M.-Y.; Yang, W.-T.; Xu, F.-J. Biocleavable Comb-Shaped Gene Carriers from Dextran Backbones with Bioreducible ATRP Initiation Sites. *Biomaterials* **2012**, *33* (6), 1873–1883.
(19) Bhattarai, N.; Ramay, H. R.; Gunn, J.; Matsen, F. A.; Zhang, M. PEG-Grafted Chitosan as an Injectable Thermosensitive Hydrogel for Sustained Protein Release. *J. Controlled Release* **2005**, *103* (3), 609–624.
(20) Seelbach, R. J.; Fransen, P.; Peroglio, M.; Pulido, D.; Lopez-Chicon, P.; Duttenhoefer, F.; Sauerbier, S.; Freiman, T.; Niemeyer, P.; Semino, C.; et al.

Multivalent Dendrimers Presenting Spatially Controlled Clusters of Binding Epitopes in Thermoresponsive Hyaluronan Hydrogels. *Acta Biomater.* **2014**, *10* (10), 4340–4350.
(21) Xu, F. J.; Ping, Y.; Ma, J.; Tang, G. P.; Yang, W. T.; Li, J.; Kang, E. T.; Neoh, K. G. Comb-Shaped Copolymers Composed of Hydroxypropyl Cellulose Backbones and Cationic Poly((2-Dimethyl Amino)Ethyl Methacrylate) Side Chains for Gene Delivery. *Bioconjug. Chem.* **2009**, *20* (8), 1449–1458.
(22) Ping, Y.; Liu, C.-D.; Tang, G.-P.; Li, J.-S.; Li, J.; Yang, W.-T.; Xu, F.-J. Functionalization of Chitosan via Atom Transfer Radical Polymerization for Gene Delivery. *Adv. Funct. Mater.* **2010**, *20* (18), 3106–3116.
(23) Tan, S.; Zhao, D.; Yuan, D.; Wang, H.; Tu, K.; Wang, L.-Q. Influence of Indomethacin-Loading on the Micellization and Drug Release of Thermosensitive Dextran-Graft-Poly(N-Isopropylacrylamide). *React. Funct. Polym.* **2011**, *71* (8), 820–827.
(24) Li, G.; Meng, Y.; Guo, L.; Zhang, T.; Liu, J. Formation of Thermo-Sensitive Polyelectrolyte Complex Micelles from Two Biocompatible Graft Copolymers for Drug Delivery. *J. Biomed. Mater. Res. A* **2014**, *102* (7), 2163–2172.
(25) Mortisen, D.; Peroglio, M.; Alini, M.; Eglin, D. Tailoring Thermoreversible Hyaluronan Hydrogels by "Click" Chemistry and RAFT Polymerization for Cell and Drug Therapy. *Biomacromolecules* **2010**, *11* (5), 1261–1272.
(26) D'Este, M.; Alini, M.; Eglin, D. Single Step Synthesis and Characterization of Thermoresponsive Hyaluronan Hydrogels. *Carbohydr. Polym.* **2012**, *90* (3), 1378–1385.
(27) Pasale, S. K.; Cerroni, B.; Ghugare, S. V.; Paradossi, G. Multiresponsive Hyaluronan-p(NiPAAm) "Click"-Linked Hydrogels. *Macromol. Biosci.* **2014**, *14* (7), 1025–1038.
(28) D'Souza, A. J. M.; Topp, E. M. Release from Polymeric Prodrugs: Linkages and Their Degradation. *J. Pharm. Sci.* **2004**, *93* (8), 1962–1979.
(29) Gillies, E. R.; Goodwin, A. P.; Fréchet, J. M. J. Acetals as PH-Sensitive Linkages for Drug Delivery. *Bioconjug. Chem.* **2004**, *15* (6), 1254–1263.
(30) Kalia, J.; Raines, R. T. Hydrolytic Stability of Hydrazones and Oximes. *Angew. Chem. Int. Ed.* **2008**, *47* (39), 7523–7526.
(31) Mahato, R.; Tai, W.; Cheng, K. Prodrugs for Improving Tumor Targetability and Efficiency. *Adv. Drug Deliv. Rev.* **2011**, *63* (8), 659–670.
(32) Pitt, C. G.; Shah, S. S. Manipulation of the Rate of Hydrolysis of Polymer-Drug Conjugates: The Degree of Hydration. *J. Controlled Release* **1995**, *33* (3), 397–403.
(33) Kondo, S.; Sasai, Y.; Kuzuya, M.; Furukawa, S. Synthesis of Water-Soluble Polymeric Prodrugs Possessing 4-Methylcatechol Derivatives by Mechanochemical Solid-State Copolymerization and Nature of Drug Release. *Chem. Pharm. Bull. (Tokyo)* **2002**, *50* (11), 1434–1438.
(34) Larsen, C. Macromolecular Prodrugs. XII. Kinetics of Release of Naproxen from Various Polysaccharide Ester Prodrugs in Neutral and Alkaline Solution. *Int. J. Pharm.* **1989**, *51* (3), 233–240.
(35) Schwartz, D. M.; Shuster, S.; Jumper, M. D.; Chang, A.; Stern, R. Human Vitreous Hyaluronidase: Isolation and Characterization. *Curr. Eye Res.* **1996**, *15* (12), 1156–1162.
(36) Delplace, V.; Payne, S.; Shoichet, M. Delivery Strategies for Treatment of Age-Related Ocular Diseases: From a Biological Understanding to Biomaterial Solutions. *J. Controlled Release* **2015**, *219*, 652–668.
(37) Age-Related Macular Degeneration (AMD) | National Eye Institute https://nei.nih.gov/eyedata/amd (accessed Nov 24, 2017).
(38) Colijn, J. M.; Buitendijk, G. H. S.; Prokofyeva, E.; Alves, D.; Cachulo, M. L.; Khawaja, A. P.; Cougnard-Gregoire, A.; Merle, B. M. J.; Korb, C.; Erke, M. G.; et al. Prevalence of Age-Related Macular Degeneration in Europe: The Past and the Future. *Ophthalmology* **2017**, *124* (12), 1753–1763.

(39) Stewart, M. W. The Expanding Role of Vascular Endothelial Growth Factor Inhibitors in Ophthalmology. *Mayo Clin. Proc.* **2012**, *87* (1), 77–88.
(40) Bhutto, I.; Lutty, G. Understanding Age-Related Macular Degeneration (AMD): Relationships between the Photoreceptor/Retinal Pigment Epithelium/Bruch's Membrane/Choriocapillaris Complex. *Mol. Aspects Med.* **2012**, *33* (4), 295–317.
(41) Kauppinen, A. From Protein Aggregation to Inflammasome Activation in RPE Cells. *Acta Ophthalmol. (Copenh.)* **2014**, *92*, 0.
(42) Bhattacharya, M.; Sarkhel, S.; Peltoniemi, J.; Broadbridge, R.; Tuomainen, M.; Auriola, S.; Urtti, A. Differentially Cleaving Peptides as a Strategy for Controlled Drug Release in Human Retinal Pigment Epithelial Cells. *J. Controlled Release* **2017**, *251*, 37–48.
(43) Kompella, U. B.; Amrite, A. C.; Pacha Ravi, R.; Durazo, S. A. Nanomedicines for Back of the Eye Drug Delivery, Gene Delivery, and Imaging. *Prog. Retin. Eye Res.* **2013**, *36*, 172–198.
(44) Platania, C. B. M.; Di Paola, L.; Leggio, G. M.; Romano, G. L.; Drago, F.; Salomone, S.; Bucolo, C. Molecular Features of Interaction between VEGFA and Anti-Angiogenic Drugs Used in Retinal Diseases: A Computational Approach. *Front. Pharmacol.* **2015**, *6*, 248.
(45) Urtti, A. Challenges and Obstacles of Ocular Pharmacokinetics and Drug Delivery. *Adv. Drug Deliv. Rev.* **2006**, *58* (11), 1131–1135.
(46) Thrimawithana, T. R.; Young, S.; Bunt, C. R.; Green, C.; Alany, R. G. Drug Delivery to the Posterior Segment of the Eye. *Drug Discov. Today* **2011**, *16* (5–6), 270–277.
(47) Nguyen, D. H.; Luo, J.; Zhang, K.; Zhang, M. Current Therapeutic Approaches in Neovascular Age-Related Macular Degeneration. *Discov. Med.* **2013**, *15* (85), 343–348.
(48) Zulliger, R.; Conley, S. M.; Naash, M. I. Non-Viral Therapeutic Approaches to Ocular Diseases: An Overview and Future Directions. *J. Controlled Release* **2015**, *219*, 471–487.
(49) del Amo, E. M.; Rimpelä, A.-K.; Heikkinen, E.; Kari, O. K.; Ramsay, E.; Lajunen, T.; Schmitt, M.; Pelkonen, L.; Bhattacharya, M.; Richardson, D.; et al. Pharmacokinetic Aspects of Retinal Drug Delivery. *Prog. Retin. Eye Res.* **2017**, *57*, 134–185.
(50) Ranta, V.-P.; Urtti, A. Transscleral Drug Delivery to the Posterior Eye: Prospects of Pharmacokinetic Modeling. *Adv. Drug Deliv. Rev.* **2006**, *58* (11), 1164–1181.
(51) Park, J.; Bungay, P. M.; Lutz, R. J.; Augsburger, J. J.; Millard, R. W.; Sinha Roy, A.; Banerjee, R. K. Evaluation of Coupled Convective–diffusive Transport of Drugs Administered by Intravitreal Injection and Controlled Release Implant. *J. Controlled Release* **2005**, *105* (3), 279–295.
(52) del Amo, E. M.; Vellonen, K.-S.; Kidron, H.; Urtti, A. Intravitreal Clearance and Volume of Distribution of Compounds in Rabbits: In Silico Prediction and Pharmacokinetic Simulations for Drug Development. *Eur. J. Pharm. Biopharm.* **2015**, *95*, *Part B*, 215–226.
(53) Shatz, W.; Hass, P. E.; Mathieu, M.; Kim, H. S.; Leach, K.; Zhou, M.; Crawford, Y.; Shen, A.; Wang, K.; Chang, D. P.; et al. Contribution of Antibody Hydrodynamic Size to Vitreal Clearance Revealed through Rabbit Studies Using a Species-Matched Fab. *Mol. Pharm.* **2016**, *13* (9), 2996–3003.
(54) Necas, J.; Bartosikova, L.; Kolar, J. Hyaluronic Acid (Hyaluronan): A Review. *Vet. Med. (Praha)* **2008**, *53* (8), 397–411.
(55) Xu, Q.; Boylan, N. J.; Suk, J. S.; Wang, Y.-Y.; Nance, E. A.; Yang, J.-C.; McDonnell, P. J.; Cone, R. A.; Duh, E. J.; Hanes, J. Nanoparticle Diffusion in, and Microrheology of, the Bovine Vitreous Ex Vivo. *J. Controlled Release* **2013**, *167* (1), 76–84.

(56) Gan, L.; Wang, J.; Zhao, Y.; Chen, D.; Zhu, C.; Liu, J.; Gan, Y. Hyaluronan-Modified Core–shell Liponanoparticles Targeting CD44-Positive Retinal Pigment Epithelium Cells via Intravitreal Injection. *Biomaterials* **2013**, *34* (24), 5978–5987.
(57) Bourges, J. L.; Bloquel, C.; Thomas, A.; Froussart, F.; Bochot, A.; Azan, F.; Gurny, R.; BenEzra, D.; Behar-Cohen, F. Intraocular Implants for Extended Drug Delivery: Therapeutic Applications. *Adv. Drug Deliv. Rev.* **2006**, *58* (11), 1182–1202.
(58) Kirchhof, S.; Goepferich, A. M.; Brandl, F. P. Hydrogels in Ophthalmic Applications. *Eur. J. Pharm. Biopharm.* **2015**, *95* (Part B), 227–238.
(59) Hennig, R.; Goepferich, A. Nanoparticles for the Treatment of Ocular Neovascularizations. *Eur. J. Pharm. Biopharm.* **2015**, *95*, *Part B*, 294–306.
(60) London, N. J. S.; Chiang, A.; Haller, J. A. The Dexamethasone Drug Delivery System: Indications and Evidence. *Adv. Ther.* **2011**, *28* (5), 351–366.
(61) Whitcup, S. M.; Robinson, M. R. Development of a Dexamethasone Intravitreal Implant for the Treatment of Noninfectious Posterior Segment Uveitis. *Ann. N. Y. Acad. Sci.* **2015**, *1358* (1), 1–12.
(62) Haller, J. A.; Bandello, F.; Belfort Jr, R.; Blumenkranz, M. S.; Gillies, M.; Heier, J.; Loewenstein, A.; Yoon, Y. H.; Jiao, J.; Li, X.-Y.; et al. Dexamethasone Intravitreal Implant in Patients with Macular Edema Related to Branch or Central Retinal Vein Occlusion: Twelve-Month Study Results. *Ophthalmology* **2011**, *118* (12), 2453–2460.
(63) Sakurai, E.; Ozeki, H.; Kunou, N.; Ogura, Y. Effect of Particle Size of Polymeric Nanospheres on Intravitreal Kinetics. *Ophthalmic Res.* **2001**, *33* (1), 31–36.
(64) Kompella, U. B.; Bandi, N.; Ayalasomayajula, S. P. Subconjunctival Nano- and Microparticles Sustain Retinal Delivery of Budesonide, a Corticosteroid Capable of Inhibiting VEGF Expression. *Invest. Ophthalmol. Vis. Sci.* **2003**, *44* (3), 1192–1201.
(65) Andrés-Guerrero, V.; Zong, M.; Ramsay, E.; Rojas, B.; Sarkhel, S.; Gallego, B.; de Hoz, R.; Ramírez, A. I.; Salazar, J. J.; Triviño, A.; et al. Novel Biodegradable Polyesteramide Microspheres for Controlled Drug Delivery in Ophthalmology. *J. Controlled Release* **2015**, *211*, 105–117.
(66) Hamdi, Y.; Lallemand, F.; Benita, S. Drug-Loaded Nanocarriers for Back-of-the-Eye Diseases- Formulation Limitations. *J. Drug Deliv. Sci. Technol.* **2015**, *30*, *Part B*, 331–341.
(67) Singh, S. R.; Grossniklaus, H. E.; Kang, S. J.; Edelhauser, H. F.; Ambati, B. K.; Kompella, U. B. Intravenous Transferrin, RGD Peptide and Dual-Targeted Nanoparticles Enhance Anti-VEGF Intraceptor Gene Delivery to Laser-Induced CNV. *Gene Ther.* **2009**, *16* (5), 645–659.
(68) Mo, Y.; Barnett, M. E.; Takemoto, D.; Davidson, H.; Kompella, U. B. Human Serum Albumin Nanoparticles for Efficient Delivery of Cu, Zn Superoxide Dismutase Gene. *Mol. Vis.* **2007**, *13*, 746–757.
(69) Suen, W.-L. L.; Chau, Y. Specific Uptake of Folate-Decorated Triamcinolone-Encapsulating Nanoparticles by Retinal Pigment Epithelium Cells Enhances and Prolongs Antiangiogenic Activity. *J. Controlled Release* **2013**, *167* (1), 21–28.
(70) Suen, W.-L. L.; Chau, Y. Size-Dependent Internalisation of Folate-Decorated Nanoparticles via the Pathways of Clathrin and Caveolae-Mediated Endocytosis in ARPE-19 Cells. *J. Pharm. Pharmacol.* **2014**, *66* (4), 564–573.
(71) Martens, T. F.; Remaut, K.; Deschout, H.; Engbersen, J. F. J.; Hennink, W. E.; van Steenbergen, M. J.; Demeester, J.; De Smedt, S. C.; Braeckmans, K. Coating Nanocarriers with Hyaluronic Acid Facilitates Intravitreal Drug Delivery for Retinal Gene Therapy. *J. Controlled Release* **2015**, *202*, 83–92.
(72) Kogan, G.; Šoltés, L.; Stern, R.; Gemeiner, P. Hyaluronic Acid: A Natural Biopolymer with a Broad Range of Biomedical and Industrial Applications. *Biotechnol. Lett.* **2007**, *29* (1), 17–25.
(73) Schanté, C. E.; Zuber, G.; Herlin, C.; Vandamme, T. F. Chemical Modifications of Hyaluronic Acid for the Synthesis of Derivatives for a Broad Range of Biomedical Applications. *Carbohydr. Polym.* **2011**, *85* (3), 469–489.

(74) Schatz, C.; Lecommandoux, S. Polysaccharide-Containing Block Copolymers: Synthesis, Properties and Applications of an Emerging Family of Glycoconjugates. *Macromol. Rapid Commun.* **2010**, *31* (19), 1664–1684.
(75) Stern, R.; Kogan, G.; Jedrzejas, M. J.; Šoltés, L. The Many Ways to Cleave Hyaluronan. *Biotechnol. Adv.* **2007**, *25* (6), 537–557.
(76) Maleki, A.; Kjøniksen, A.-L.; Nyström, B. Effect of PH on the Behavior of Hyaluronic Acid in Dilute and Semidilute Aqueous Solutions. *Macromol. Symp.* **2008**, *274* (1), 131–140.
(77) Huin-Amargier, C.; Marchal, P.; Payan, E.; Netter, P.; Dellacherie, E. New Physically and Chemically Crosslinked Hyaluronate (HA)-Based Hydrogels for Cartilage Repair. *J. Biomed. Mater. Res. A* **2006**, *76A* (2), 416–424.
(78) Li, J.; Huang, P.; Chang, L.; Long, X.; Dong, A.; Liu, J.; Chu, L.; Hu, F.; Liu, J.; Deng, L. Tumor Targeting and PH-Responsive Polyelectrolyte Complex Nanoparticles Based on Hyaluronic Acid-Paclitaxel Conjugates and Chitosan for Oral Delivery of Paclitaxel. *Macromol. Res.* **2013**, *21* (12), 1331–1337.
(79) Purcell, B. P.; Kim, I. L.; Chuo, V.; Guenin, T.; Dorsey, S. M.; Burdick, J. A. Incorporation of Sulfated Hyaluronic Acid Macromers into Degradable Hydrogel Scaffolds for Sustained Molecule Delivery. *Biomater. Sci.* **2014**, *2*, 693–702.
(80) Pravata, L.; Braud, C.; Boustta, M.; El Ghzaoui, A.; Tømmeraas, K.; Guillaumie, F.; Schwach-Abdellaoui, K.; Vert, M. New Amphiphilic Lactic Acid Oligomer−Hyaluronan Conjugates: Synthesis and Physicochemical Characterization. *Biomacromolecules* **2008**, *9* (1), 340–348.
(81) Yeom, J.; Bhang, S. H.; Kim, B.-S.; Seo, M. S.; Hwang, E. J.; Cho, I. H.; Park, J. K.; Hahn, S. K. Effect of Cross-Linking Reagents for Hyaluronic Acid Hydrogel Dermal Fillers on Tissue Augmentation and Regeneration. *Bioconjug. Chem.* **2010**, *21* (2), 240–247.
(82) Schanté, C. E.; Zuber, G.; Herlin, C.; Vandamme, T. F. Improvement of Hyaluronic Acid Enzymatic Stability by the Grafting of Amino-Acids. *Carbohydr. Polym.* **2012**, *87* (3), 2211–2216.
(83) Laurent, U. B. G.; Fraser, J. R. E. Turnover of Hyaluronate in the Aqueous Humour and Vitreous Body of the Rabbit. *Exp. Eye Res.* **1983**, *36* (4), 493–503.
(84) Kolb, H. C.; Finn, M. G.; Sharpless, K. B. Click Chemistry: Diverse Chemical Function from a Few Good Reactions. *Angew. Chem. Int. Ed.* **2001**, *40* (11), 2004–2021.
(85) Espeel, P.; Du Prez, F. E. "Click"-Inspired Chemistry in Macromolecular Science: Matching Recent Progress and User Expectations. *Macromolecules* **2015**, *48* (1), 2–14.
(86) Crescenzi, V.; Cornelio, L.; Di Meo, C.; Nardecchia, S.; Lamanna, R. Novel Hydrogels via Click Chemistry: Synthesis and Potential Biomedical Applications. *Biomacromolecules* **2007**, *8* (6), 1844–1850.
(87) Bencherif, S. A.; Washburn, N. R.; Matyjaszewski, K. Synthesis by AGET ATRP of Degradable Nanogel Precursors for In Situ Formation of Nanostructured Hyaluronic Acid Hydrogel. *Biomacromolecules* **2009**, *10* (9), 2499–2507.
(88) Famili, A.; Rajagopal, K. Bio-Orthogonal Cross-Linking Chemistry Enables In Situ Protein Encapsulation and Provides Sustained Release from Hyaluronic Acid Based Hydrogels. *Mol. Pharm.* **2017**, *14* (6), 1961–1968.
(89) Narain, R. *Chemistry of Bioconjugates : Synthesis, Characterization, and Biomedical Applications*, 1st ed.; Wiley: Somerset, United States, 2013.
(90) Bulpitt, P.; Aeschlimann, D. New Strategy for Chemical Modification of Hyaluronic Acid: Preparation of Functionalized Derivatives and Their Use in the Formation of Novel Biocompatible Hydrogels. *J. Biomed. Mater. Res.* **1999**, *47* (2), 152–169.
(91) Bergman, K.; Elvingson, C.; Hilborn, J.; Svensk, G.; Bowden, T. Hyaluronic Acid Derivatives Prepared in Aqueous Media by Triazine-Activated Amidation. *Biomacromolecules* **2007**, *8* (7), 2190–2195.

(92) D'Este, M.; Eglin, D.; Alini, M. A Systematic Analysis of DMTMM vs EDC/NHS for Ligation of Amines to Hyaluronan in Water. *Carbohydr. Polym.* **2014**, *108* (Supplement C), 239–246.
(93) Bencherif, S. A.; Srinivasan, A.; Horkay, F.; Hollinger, J. O.; Matyjaszewski, K.; Washburn, N. R. Influence of the Degree of Methacrylation on Hyaluronic Acid Hydrogels Properties. *Biomaterials* **2008**, *29* (12), 1739–1749.
(94) Manju, S.; Sreenivasan, K. Conjugation of Curcumin onto Hyaluronic Acid Enhances Its Aqueous Solubility and Stability. *J. Colloid Interface Sci.* **2011**, *359* (1), 318–325.
(95) Hirano, K.; Sakai, S.; Ishikawa, T.; Avci, F. Y.; Linhardt, R. J.; Toida, T. Preparation of the Methyl Ester of Hyaluronan and Its Enzymatic Degradation. *Carbohydr. Res.* **2005**, *340* (14), 2297–2304.
(96) Pelletier, S.; Hubert, P.; Lapicque, F.; Payan, E.; Dellacherie, E. Amphiphilic Derivatives of Sodium Alginate and Hyaluronate: Synthesis and Physico-Chemical Properties of Aqueous Dilute Solutions. *Carbohydr. Polym.* **2000**, *43* (4), 343–349.
(97) Della, V.; Romeo, A. New Polysaccharide Esters and Their Salts. EP0216453 (A2), April 1, 1987.
(98) Campoccia, D.; Doherty, P.; Radice, M.; Brun, P.; Abatangelo, G.; Williams, D. F. Semisynthetic Resorbable Materials from Hyaluronan Esterification. *Biomaterials* **1998**, *19* (23), 2101–2127.
(99) Balazs, E. A. Therapeutic Use of Hyaluronan. *Struct. Chem.* **2009**, *20* (2), 341–349.
(100) Jui-Yang Lai; David Hui-Kang Ma; Hsiao-Yun Cheng; Chi-Chin Sun; Shu-Jung Huang; Ya-Ting Li; Ging-Ho Hsiue. Ocular Biocompatibility of Carbodiimide Cross-Linked Hyaluronic Acid Hydrogels for Cell Sheet Delivery Carriers. *J. Biomater. Sci. -- Polym. Ed.* **2010**, *21* (3), 359–376.
(101) Soiberman, U.; Kambhampati, S. P.; Wu, T.; Mishra, M. K.; Oh, Y.; Sharma, R.; Wang, J.; Al Towerki, A. E.; Yiu, S.; Stark, W. J.; et al. Subconjunctival Injectable Dendrimer-Dexamethasone Gel for the Treatment of Corneal Inflammation. *Biomaterials* **2017**, *125* (Supplement C), 38–53.
(102) Martens, T. F.; Peynshaert, K.; Nascimento, T. L.; Fattal, E.; Karlstetter, M.; Langmann, T.; Picaud, S.; Demeester, J.; De Smedt, S. C.; Remaut, K.; et al. Effect of Hyaluronic Acid-Binding to Lipoplexes on Intravitreal Drug Delivery for Retinal Gene Therapy. *Eur. J. Pharm. Sci.* **2017**, *103*, 27–35.
(103) Yadav, A. K.; Mishra, P.; Agrawal, G. P. An Insight on Hyaluronic Acid in Drug Targeting and Drug Delivery. *J. Drug Target.* **2008**, *16* (2), 91–107.
(104) Knop, K.; Hoogenboom, R.; Fischer, D.; Schubert, U. S. Poly(Ethylene Glycol) in Drug Delivery: Pros and Cons as Well as Potential Alternatives. *Angew. Chem. Int. Ed.* **2010**, *49* (36), 6288–6308.
(105) Pasut, G.; Veronese, F. M. Polymer–drug Conjugation, Recent Achievements and General Strategies. *Prog. Polym. Sci.* **2007**, *32* (8–9), 933–961.
(106) Pelegri-O'Day, E. M.; Lin, E.-W.; Maynard, H. D. Therapeutic Protein–Polymer Conjugates: Advancing Beyond PEGylation. *J. Am. Chem. Soc.* **2014**, *136* (41), 14323–14332.
(107) van Witteloostuijn, S. B.; Pedersen, S. L.; Jensen, K. J. Half-Life Extension of Biopharmaceuticals Using Chemical Methods: Alternatives to PEGylation. *ChemMedChem* **2016**, *11* (22), 2474–2495.
(108) Obermeier, B.; Wurm, F.; Mangold, C.; Frey, H. Multifunctional Poly(Ethylene Glycol)S. *Angew. Chem. Int. Ed.* **2011**, *50* (35), 7988–7997.
(109) Thomas, A.; Müller, S. S.; Frey, H. Beyond Poly(Ethylene Glycol): Linear Polyglycerol as a Multifunctional Polyether for Biomedical and Pharmaceutical Applications. *Biomacromolecules* **2014**, *15* (6), 1935–1954.
(110) Kainthan, R. K.; Janzen, J.; Levin, E.; Devine, D. V.; Brooks, D. E. Biocompatibility Testing of Branched and Linear Polyglycidol. *Biomacromolecules* **2006**, *7* (3), 703–709.

(111) Weinhart, M.; Becherer, T.; Schnurbusch, N.; Schwibbert, K.; Kunte, H.-J.; Haag, R. Linear and Hyperbranched Polyglycerol Derivatives as Excellent Bioinert Glass Coating Materials. *Adv. Eng. Mater.* **2011**, *13* (12), B501–B510.
(112) Imran ul-haq, M.; Lai, B. F. L.; Chapanian, R.; Kizhakkedathu, J. N. Influence of Architecture of High Molecular Weight Linear and Branched Polyglycerols on Their Biocompatibility and Biodistribution. *Biomaterials* **2012**, *33* (35), 9135–9147.
(113) Brocas, A.-L.; Mantzaridis, C.; Tunc, D.; Carlotti, S. Polyether Synthesis: From Activated or Metal-Free Anionic Ring-Opening Polymerization of Epoxides to Functionalization. *Prog. Polym. Sci.* **2013**, *38* (6), 845–873.
(114) Erberich, M.; Keul, H.; Möller, M. Polyglycidols with Two Orthogonal Protective Groups: Preparation, Selective Deprotection, and Functionalization. *Macromolecules* **2007**, *40* (9), 3070–3079.
(115) Obermeier, B.; Frey, H. Poly(Ethylene Glycol-Co-Allyl Glycidyl Ether)s: A PEG-Based Modular Synthetic Platform for Multiple Bioconjugation. *Bioconjug. Chem.* **2011**, *22* (3), 436–444.
(116) Deffieux, A.; Carlotti, S.; Barrère, A. 4.07 - Anionic Ring-Opening Polymerization of Epoxides and Related Nucleophilic Polymerization Processes. In *Polymer Science: A Comprehensive Reference*; Matyjaszewski, K., Möller, M., Eds.; Elsevier: Amsterdam, 2012; pp 117–140.
(117) Billouard, C.; Carlotti, S.; Desbois, P.; Deffieux, A. "Controlled" High-Speed Anionic Polymerization of Propylene Oxide Initiated by Alkali Metal Alkoxide/Trialkylaluminum Systems. *Macromolecules* **2004**, *37* (11), 4038–4043.
(118) Carlotti, S.; Billouard, C.; Gautriaud, E.; Desbois, P.; Deffieux, A. Activation Mechanisms of Trialkylaluminum in Alkali Metal Alkoxides or Tetraalkylammonium Salts / Propylene Oxide Controlled Anionic Polymerization. *Macromol. Symp.* **2005**, *226* (1), 61–68.
(119) Labbé, A.; Carlotti, S.; Billouard, C.; Desbois, P.; Deffieux, A. Controlled High-Speed Anionic Polymerization of Propylene Oxide Initiated by Onium Salts in the Presence of Triisobutylaluminum. *Macromolecules* **2007**, *40* (22), 7842–7847.
(120) Gervais, M.; Labbé, A.; Carlotti, S.; Deffieux, A. Direct Synthesis of α-Azido,ω-Hydroxypolyethers by Monomer-Activated Anionic Polymerization. *Macromolecules* **2009**, *42* (7), 2395–2400.
(121) Dworak, A.; Panchev, I.; Trzebicka, B.; Walach, W. Poly(α-t-Butoxy-ω-Styrylo-Glycidol): A New Reactive Surfactant. *Polym. Bull.* **1998**, *40* (4–5), 461–468.
(122) Thomas, A.; Niederer, K.; Wurm, F.; Frey, H. Combining Oxyanionic Polymerization and Click-Chemistry: A General Strategy for the Synthesis of Polyether Polyol Macromonomers. *Polym. Chem.* **2013**, *5* (3), 899–909.
(123) Dworak, A.; Trzebicka, B.; Utrata, A.; Walach, W. Hydrophobically Modified Polyglycidol – the Control of Lower Critical Solution Temperature. *Polym. Bull.* **2003**, *50* (1–2), 47–54.
(124) Stiriba, S.-E.; Kautz, H.; Frey, H. Hyperbranched Molecular Nanocapsules: Comparison of the Hyperbranched Architecture with the Perfect Linear Analogue. *J. Am. Chem. Soc.* **2002**, *124* (33), 9698–9699.
(125) Groll, J.; Singh, S.; Albrecht, K.; Moeller, M. Biocompatible and Degradable Nanogels via Oxidation Reactions of Synthetic Thiomers in Inverse Miniemulsion. *J. Polym. Sci. Part Polym. Chem.* **2009**, *47* (20), 5543–5549.
(126) Li, Z.; Chau, Y. Synthesis of Linear Polyether Polyol Derivatives As New Materials for Bioconjugation. *Bioconjug. Chem.* **2009**, *20* (4), 780–789.
(127) Kunishima, M.; Kawachi, C.; Monta, J.; Terao, K.; Iwasaki, F.; Tani, S. 4-(4,6-Dimethoxy-1,3,5-Triazin-2-Yl)-4-Methyl-Morpholinium Chloride: An Efficient Condensing Agent Leading to the Formation of Amides and Esters. *Tetrahedron* **1999**, *55* (46), 13159–13170.
(128) Nishikubo, T.; Kameyama, A.; Yamada, Y.; Yoshida, Y. Synthesis of Polymers in Aqueous Solutions: Esterification Reaction of Poly(Methacrylic Acid) with Alkyl

Halides Using DBU in Aqueous Solutions. *J. Polym. Sci. Part Polym. Chem.* **1996**, *34* (17), 3531–3537.
(129) Wurm, F.; Nieberle, J.; Frey, H. Synthesis and Characterization of Poly(Glyceryl Glycerol) Block Copolymers. *Macromolecules* **2008**, *41* (6), 1909–1911.
(130) Liu, X.-M.; Quan, L.; Tian, J.; Laquer, F. C.; Ciborowski, P.; Wang, D. Syntheses of Click PEG−Dexamethasone Conjugates for the Treatment of Rheumatoid Arthritis. *Biomacromolecules* **2010**, *11* (10), 2621–2628.
(131) Kamiński, Z. J. The Concept of Superactive Esters. *Int. J. Pept. Protein Res.* **1994**, *43* (3), 312–319.
(132) Gervais, M.; Brocas, A.-L.; Cendejas, G.; Deffieux, A.; Carlotti, S. Synthesis of Linear High Molar Mass Glycidol-Based Polymers by Monomer-Activated Anionic Polymerization. *Macromolecules* **2010**, *43* (4), 1778–1784.
(133) Baumann, A.; Tuerck, D.; Prabhu, S.; Dickmann, L.; Sims, J. Pharmacokinetics, Metabolism and Distribution of PEGs and PEGylated Proteins: Quo Vadis? *Drug Discov. Today* **2014**, *19* (10), 1623–1631.
(134) Cash, J. J.; Kubo, T.; Bapat, A. P.; Sumerlin, B. S. Room-Temperature Self-Healing Polymers Based on Dynamic-Covalent Boronic Esters. *Macromolecules* **2015**, *48* (7), 2098–2106.
(135) Marinaro, W. A.; Prankerd, R.; Kinnari, K.; Stella, V. J. Interaction of Model Aryl- and Alkyl-Boronic Acids and 1,2-Diols in Aqueous Solution. *J. Pharm. Sci.* **2015**, *104* (4), 1399–1408.
(136) Šoltés, L.; Valachová, K.; Mendichi, R.; Kogan, G.; Arnhold, J.; Gemeiner, P. Solution Properties of High-Molar-Mass Hyaluronans: The Biopolymer Degradation by Ascorbate. *Carbohydr. Res.* **2007**, *342* (8), 1071–1077.
(137) Payan, E.; Jouzeau, J. Y.; Lapicque, F.; Bordji, K.; Simon, G.; Gillet, P.; O'Regan, M.; Netter, P. In Vitro Drug Release from HYC 141, a Corticosteroid Ester of High Molecular Weight Hyaluronan. *J. Controlled Release* **1995**, *34* (2), 145–153.